Renormalization and embedded Julia sets in the Mandelbrot set

Wolf Jung
Gesamtschule Brand, 52078 Aachen, Germany.
E-mail: jung@mndynamics.com

Abstract

The decorations of a small Mandelbrot set within the Mandelbrot set $\mathcal{M}$ contain embedded Julia sets; these are Cantor sets quasiconformally homeomorphic to a quadratic Julia set. So the local geometry of $\mathcal{M}$ shows the shape of corresponding Julia sets. This phenomenon was observed in the 1990s by Munafo and others. Families of embedded Julia sets were obtained analytically by Douady et alii and by Kawahira–Kisaka. The present paper gives an alternative construction by finding suitable puzzle-pieces with a geometric-combinatorial method.

Consider any non-parabolic parameter in the boundary of a small Mandelbrot set, e.g., a Siegel parameter . Then there is a sequence of embedded Julia sets converging to this parameter, whose asymptotic geometry is a conformal copy of the small filled Julia set.

The structure of the Mandelbrot set at an embedded Julia set is described by channels and nodes, which correspond to precritical ray pairs and to precritical points for a Cantor Julia set with dyadic angle. Moreover, relations between embedded Julia sets and other similarity phenomena are explored, including notions of asymptotic and local similarity.

1 Introduction

When a complex quadratic polynomial $f_c(z) = z^2 + c$ is iterated, all points z with large $|z|$ escape to infinity, and there is a compact f_c-invariant set $\mathcal{K}_c$, the filled Julia set. Its boundary $\partial\mathcal{K}_c$ is the strict Julia set, where the dynamics is chaotic. Now either $\mathcal{K}_c$ is connected, and the orbit of the critical point $z = 0$ and critical value $z = c$ is bounded and contained in $\mathcal{K}_c$, or the critical orbit escapes and $\mathcal{K}_c$ is totally disconnected, in fact a Cantor set. In the former case, the parameter c of $f_c(z)$ belongs to the Mandelbrot set $\mathcal{M}$.

Any Julia set $\partial\mathcal{K}_c$ contains a dense family of repelling periodic and preperiodic points z, which explains its self-similarity. The Mandelbrot set shows various phenomena of self-similarity and of similarity to Julia sets as well. Probably best known are the asymptotic scaling properties at Misiurewicz points [43] and the appearance of small Mandelbrot sets $\mathcal{M}_p \subset \mathcal{M}$ [5, 18, 26], see Figure 1. For $c \in \mathcal{M}_p$, there is a small Julia set $\mathcal{K}_c^p \subset \mathcal{K}_c$, such that the p-th iterate $f_c^p(z)$ behaves like a quadratic polynomial in a neighborhood of $\mathcal{K}_c^p$. More precisely, there is a quasiconformal conjugation from the restricted $f_c^p(z)$ to a new quadratic polynomial $f_{\widehat{c}}(\widehat{z})$, which maps $\mathcal{K}_c^p$ to $\mathcal{K}_{\widehat{c}}$. The corresponding map $c \mapsto \widehat{c}$ in the parameter plane is a homeomorphism $\mathcal{M}_p \to \mathcal{M}$. Both $\mathcal{K}_c \setminus \mathcal{K}_c^p$ and $\mathcal{M} \setminus \mathcal{M}_p$ consist of a countable family of decorations. Similarity phenomena related to decorations are discussed in [19].

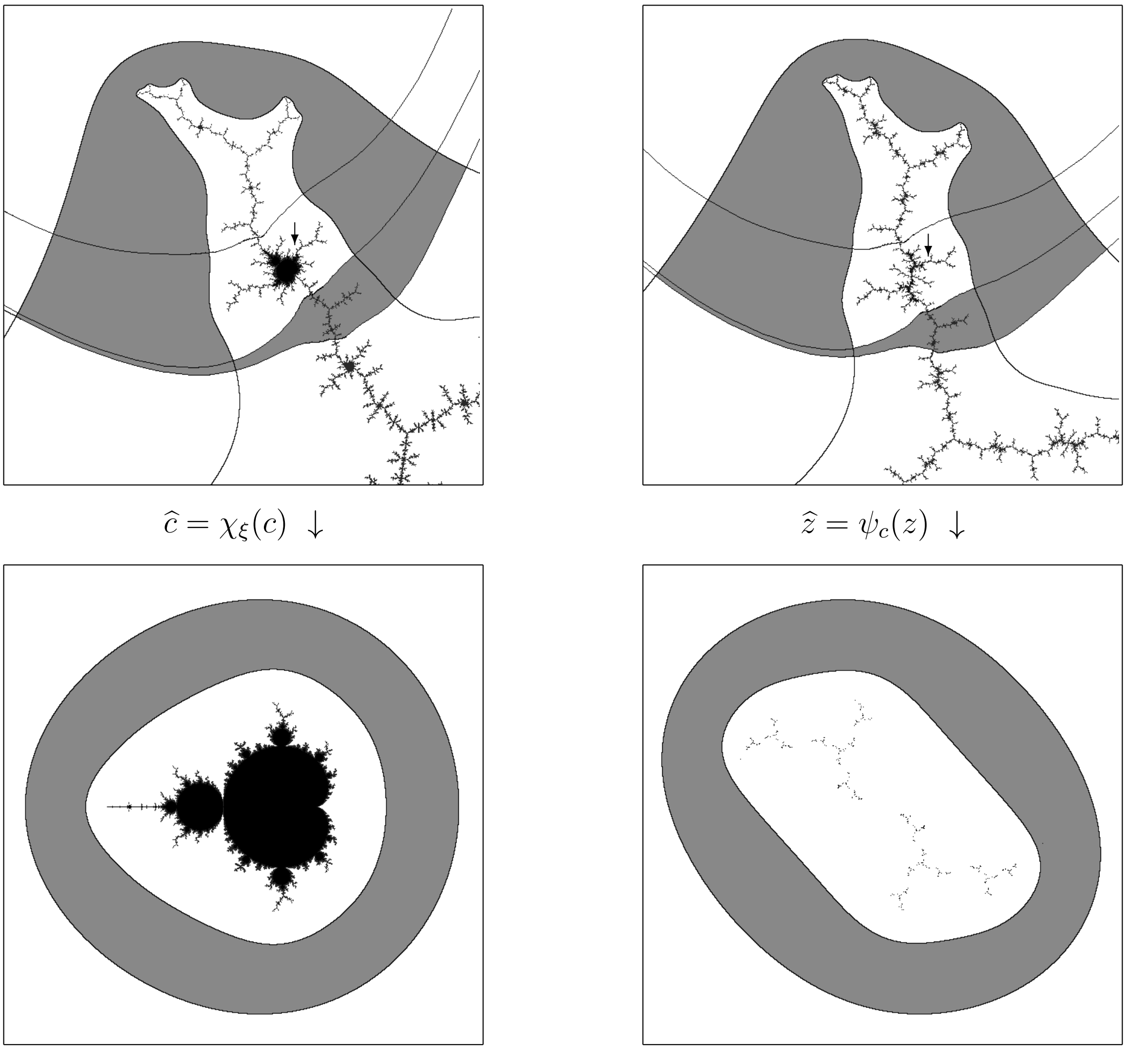

Figure 1: By renormalization and straightening, the small Mandelbrot set $\mathcal{M}_4 \subset \mathcal{M}$ is mapped to the full Mandelbrot set $\mathcal{M}$ and the small Julia set $\mathcal{K}_c^4 \subset \mathcal{K}_c$ is mapped to the filled Julia set $\mathcal{K}_{\widehat{c}}$. The fundamental annuli $U_M \setminus \overline{U_M'}$ and $U_c \setminus \overline{U_c'}$ are bounded by corresponding external rays and equipotential lines.
Here we have $c = c_{23} \in \mathcal{M} \setminus \mathcal{M}_4$, so $\mathcal{K}_c$ is connected but $\mathcal{K}_c^4$ and $\mathcal{K}_{\widehat{c}}$ are Cantor sets, and the parameter $\widehat{c} \in \mathbb{C} \setminus \mathcal{M}$ depends on the choice of the tubing ξ. Neither the embedded Julia set $\mathcal{K}_M^{23,\,4} \subset \partial\mathcal{M}$ nor $\mathcal{K}_c^{23,\,4} \subset \partial\mathcal{K}_c$ are visible on this scale; they are marked with arrows.

Embedded Julia sets were observed and named in the 1990s by Robert Munafo and Jonathan Leavitt [31, 23]. These are subsets of $\mathcal{M}$ resembling a quadratic Julia set. See the examples in Figures 2 and 10. It turns out that each embedded Julia set is associated to two small Mandelbrot sets: first, it is contained in a decoration of a small Mandelbrot set $\mathcal{M}_p$ and it looks similar to the small Julia sets $\mathcal{K}_c^p$ for parameters c nearby. Second, it is somewhat symmetric about another small

Mandelbrot set $\mathcal{M}_m$, which we shall call the tiny Mandelbrot set in this context. The embedded Julia set is denoted by $\mathcal{K}_M^{m,\,p} \subset \mathcal{M}$; of course the periods m and p do not specify $\mathcal{M}_m$, $\mathcal{M}_p$, and $\mathcal{K}_M^{m,\,p}$ uniquely, but they must be supplemented with parameter values or external angles. Now what is the mechanism producing $\mathcal{K}_M^{m,\,p}$?

- There is a p-cycle of small Julia sets for f_c^p; $\mathcal{K}_c^p$ denotes the small Julia set around the critical value $z = c$ and $f_c^{-1}(\mathcal{K}_c^p) = f_c^{p-1}(\mathcal{K}_c^p)$ is located at the critical point $z = 0$. Now these exist not only for parameters $c \in \mathcal{M}_p$ but for c in a neighborhood of $\mathcal{M}_p$; when $c \notin \mathcal{M}_p$, then $\mathcal{K}_c^p$ is a Cantor set.
- This neighborhood contains a small disk V_M around $\mathcal{M}_m$, which is disjoint from $\mathcal{M}_p$, such that: for $c \in V_M$ there is a subset $\mathcal{K}_c^{m,\,p} \subset \mathcal{K}_c$ around $z = c$, which is mapped conformally to $f_c^{-1}(\mathcal{K}_c^p)$ by $f_c^{m-1}(z)$.
- Now the embedded Julia set $\mathcal{K}_M^{m,\,p} \subset \mathcal{M}$ contains those parameters c, such that the critical value c belongs to $\mathcal{K}_c^{m,\,p}$ for this parameter.

Note that there may be more parameters c with $f_c^{m-1}(c) \in f_c^{-1}(\mathcal{K}_c^p)$, but here we assume that the set $\mathcal{K}_c^{m,\,p}$ is mapped to $\mathcal{K}_c^p$ as a whole and $f_c^{m-1}(z)$ is conformal in a neighborhood V_c. When $\mathcal{K}_M^{m,\,p}$ is close to $\mathcal{M}_p$, then it approximates a connected set with respect to the Hausdorff metric, and it looks connected in the figures when this distance is less than the pixel size. If the embedded Julia set is farther away from the small Mandelbrot set, it looks like a Cantor set supplemented with connecting arcs in the complementary channels, see Figures 9 and 11. When $\mathcal{K}_M^{m,\,p}$ is widely disconnected, it is visible only using specific colorings, but it may produce a family of branch points showing a recursive subdivision of $\mathcal{M}$.

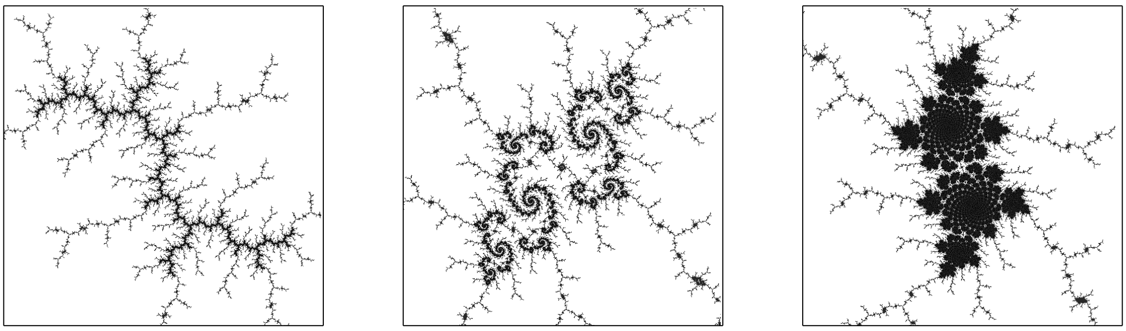

Figure 2: Embedded Julia sets $\mathcal{K}_M^{m,\,4} \subset \partial\mathcal{M}$, which are close to the small Mandelbrot set $\mathcal{M}_4$ and which surround tiny Mandelbrot sets of period m. Left: $\mathcal{K}_M^{59,\,4}$ is similar to a copy of the Misiurewicz Julia set $\mathcal{K}_{\mathrm{i}}$. Middle: $\mathcal{K}_M^{55,\,4}$ is an imploded parabolic Basilica. Right: $\mathcal{K}_M^{135,\,4}$ is close to the Siegel parameter with Golden Mean rotation number in $\mathcal{M}_4$.

The notion of embedded Julia sets provides a partial description of the geometry of the Mandelbrot set, or more specifically, of the decorations at any small Mandelbrot set. Perhaps the most intriguing aspect is the similarity to small Julia sets: when you move around the boundary of $\mathcal{M}_p$, you see that the decorations are filled with embedded sets, which look like small Julia sets $\mathcal{K}_c^p$ for the current parameters c. See also Figures 3 and 5. — The main results are stated more formally in the following Theorem A, and in Theorems B and C below:

Theorem A (Density and asymptotic geometry of embedded Julia sets) *Suppose $\mathcal{M}_p \subset \mathcal{M}$ is a primitive or satellite small Mandelbrot set of period p. For suitable parapuzzle-pieces V_M and corresponding puzzle-pieces V_c, $c \in V_M$, there is a conformal image $\mathcal{K}_c^{m,p} \subset \partial\mathcal{K}_c$ of the small Julia set $\mathcal{K}_c^p$ in V_c, such that f_c^{m-1} : $\mathcal{K}_c^{m,p} \to f_c^{p-1}(\mathcal{K}_c^p) = f_c^{-1}(\mathcal{K}_c^p)$. Then define the corresponding* ***embedded Julia set*** *$\mathcal{K}_M^{m,p} := \{c \in V_M \,|\, c \in \mathcal{K}_c^{m,p}\}$. It is a Cantor set in $\partial\mathcal{M}$ and a quasiconformal image of $\mathcal{K}_c^{m,p}$ and $\mathcal{K}_c^p$ for $c \in V_M$, with an explicit bound on the dilatation.*

For any $b \in \partial\mathcal{M}_p$ there is a sequence of embedded Julia sets $\mathcal{K}_M^{m_j,p} \subset \partial\mathcal{M}$ with $\mathcal{K}_M^{m_j,p} \to \{b\}$ as $j \to \infty$. When b is not parabolic, this sequence can be chosen such that there are affine maps A_j and $A_j(\mathcal{K}_M^{m_j,p})$ converges to a conformal copy of the small Julia set $\mathcal{K}_b^p$, which is a quasiconformal copy of $\mathcal{K}_{\widehat{b}}$.

For any $\mathcal{K}_M^{m,p}$ there is a unique primitive small Mandelbrot set $\mathcal{M}_m \subset V_M$ of period m, which shall be called the ***tiny Mandelbrot set*** *in reference to $\mathcal{M}_p$ and $\mathcal{K}_M^{m,p}$. Nested annuli around $\mathcal{M}_m$ contain embedded Julia sets $\mathcal{K}_M^{l\cdot m,p}$ of higher* ***levels*** *l, which correspond to preimages $\mathcal{K}_c^{l\cdot m,p}$ of $\mathcal{K}_c^{1\cdot m,p} = \mathcal{K}_c^{m,p}$ under $f_c^{(l-1)\cdot m}$.*

Embedded Julia sets $\mathcal{K}_M^{2\cdot m,p}$ and $\mathcal{K}_M^{3\cdot m,p}$ are shown in Figures 8 and 12. — Conceptually, the proof of the construction of $\mathcal{K}_M^{1\cdot m,p} = \mathcal{K}_M^{m,p}$ is divided into two parts:

- For a suitable disk V_M and corresponding disks V_c in the dynamic plane, $\mathcal{K}_c^p$ and $\mathcal{K}_c^{m,p}$ move holomorphically. Then Proposition 2.3 by Douady–Hubbard and Lyubich [5, 25, 26] gives a corresponding set $\mathcal{K}_M^{m,p}$ in the parameter plane and a quasiconformal homeomorphism. Following earlier applications in [41, 2], this principle was used implicitly to construct embedded Julia sets in [8, 21].

- Given $\mathcal{M}_p$ and $\mathcal{M}_m$, it is not always possible to find a suitable disk V_M; V_c must be small enough such that $f_c^{m-1}(z)$ is injective, and big enough so that $f_c^{m-1}(V_c)$ contains $f_c^{-1}(\mathcal{K}_c^p)$. Additional arguments are required to show that embedded Julia sets actually exist everywhere at $\partial\mathcal{M}_p$, see below.

Complex dynamics uses both analytic and combinatorial tools, e.g., basic results on local connectivity and landing properties of external rays can be shown alternatively by analytic methods [4] or geometric-combinatorial methods [29, 39]. The construction of small Mandelbrot sets by renormalization combines both approaches [11, 18]. So there are different methods to obtain embedded Julia sets:

- Suitable disks V_M and V_c may be constructed analytically from asymptotic expressions for $f_c^p(z)$ and $f_c^m(z)$. This was done by Douady et alii [8] using Fatou coordinates at primitive roots, and by Kawahira–Kisaka [21] at satellite roots and Misiurewicz points.

- In the present paper, suitable parapuzzle-pieces V_M and corresponding puzzle-pieces V_c are constructed combinatorially, i.e., by observing the orbit and the qualitative geometry of edges and segments on decorations.

- Both methods give sequences of embedded Julia sets converging to any root or Misiurewicz point in $\partial\mathcal{M}_p$; since these are dense, embedded Julia sets are dense at $\partial\mathcal{M}_p$. But what is more, they actually approximate copies of any small filled Julia set $\mathcal{K}_b^p$, $b \in \partial\mathcal{M}_p$, except when b is a root.

In 2008 the author obtained the combinatorial construction and the asymptotic geometry at non-parabolic parameters, as well as the similarity results in Theorem C, but this was published only in preliminary form in Demo Section 5 of Mandel [15] and remained unknown; the discoveries of [21] are completely independent. Probably the combinatorial approach is simpler for quadratic polynomials and gives more classes of examples, while the analytic approach of [8, 21] will be more easily adapted to general one-parameter families of rational maps.

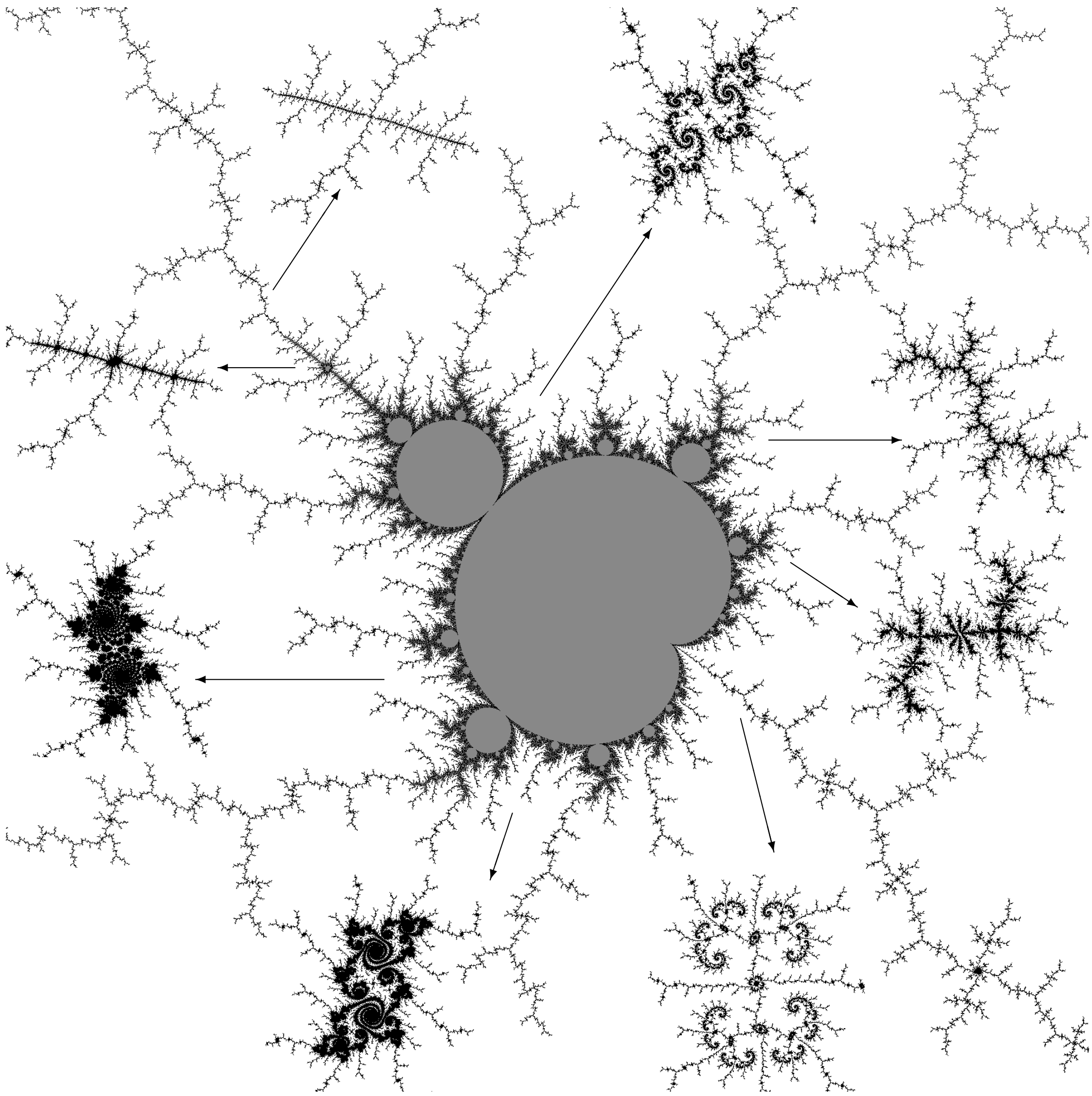

Figure 3: The small Mandelbrot set $\mathcal{M}_4$ and eight magnified images from its decorations. The embedded Julia sets show the shape of corresponding small Julia sets.

Theorem B (Structure of embedded Julia sets)
*The geometry of $\mathcal{K}_M^{m,p}$ within $\mathcal{M}$ is described by complementary channels. For each order $k \ge 0$, $\mathcal{K}_M^{m,p}$ has a dynamically natural subdivision into 2^k subsets, each of which is an embedded Julia set $\mathcal{K}_M^{m+kp,p}$ of preperiod $m + kp$. The corresponding tiny Mandelbrot sets $\mathcal{M}_{m+kp}$ are called **nodes of order** k. The Cantor set $\mathcal{K}_M^{m,p}$ is the accumulation set of the family of nodes. The external angles of the nodes are obtained by appending binary digits from the angles of $\mathcal{M}_m$ and $\mathcal{M}_p$.*

When $\mathcal{M}_m$ is behind $\mathcal{M}_p$, the channels between those subsets correspond to merged carrots of $\mathcal{K}_c^p$ and to crashing rays of $\mathcal{K}_{\widehat{c}}$. Here c is an arbitrary parameter in the decoration of internal angle θ containing $\mathcal{K}_M^{m,p}$, and $\widehat{c}$ is any parameter on the dyadic ray of angle θ. Likewise, the nodes of order k correspond to preimages of the critical point ω_c^p under f_c^{kp} and to preimages of 0 under $f_{\widehat{c}}^k$, respectively.

Accumulation of nodes was conjectured by Munafo [31] and the patterns of angles were observed by Romera et alii [37, 38]. In Section 4, embedded Julia sets are discussed in relation to other similarity phenomena [43, 19]. See also Figures 8 and 12.

Theorem C (Compatibility with various similarity phenomena)
For suitable parapuzzle-pieces P_M, quasiconformal surgery gives a homeomorphism from $\mathcal{M} \cap P_M$ onto itself; in general an embedded Julia set $\mathcal{K}_M^{m,p} \subset P_M$ will be mapped to another embedded Julia set $\mathcal{K}_M^{m',p'}$.

At any Misiurewicz point there are sequences of tiny Mandelbrot sets with geometric scaling behavior; their decorations show phenomena of asymptotic and local similarity, which apply to embedded Julia sets in particular.

Algorithms for computing images of small Mandelbrot sets and embedded Julia sets are discussed briefly in Appendix A. An excerpt of a forthcoming comprehensive paper on renormalization [18] is found in Appendix B.

Acknowledgment

Many colleagues have contributed to this work by inspiring discussions and helpful suggestions. I wish to thank in particular Arnaud Chéritat, Kostiantyn Drach, Claude Heiland-Allen, Tomoki Kawahira, Masashi Kisaka, Luna Lomonaco, Robert P. Munafo, Johannes Riedl, and Dierk Schleicher. This research was partially supported by Dierk Schleicher's ERC grant HOLOGRAM.

2 Background

See [3, 30] for a comprehensive introduction to complex dynamics. The dynamic plane and the Julia set are cut into pieces by external rays; the pieces move holomorphically with the parameter, which gives rise to various quasiconformal maps. This is useful for renormalization in general, and for the construction of embedded Julia sets in Section 3.

2.1 Quadratic polynomials

For $c \in \mathcal{M}$ the **filled Julia set** $\mathcal{K}_c$ is compact, connected, and full. The Boettcher map $\Phi_c : \widehat{\mathbb{C}} \setminus \mathcal{K}_c \to \widehat{\mathbb{C}} \setminus \overline{\mathbb{D}}$ conjugates $f_c(z) = z^2 + c$ to $F(z) = z^2$; preimages of radial lines and circles are called **dynamic rays** and **equipotential lines**, respectively. The angle of a dynamic ray is doubled under the map $f_c(z)$, and the ray is periodic or preperiodic when the angle is rational, i.e., a rational multiple of 2π; then the ray lands at a repelling or parabolic periodic or preperiodic point $z \in \partial\mathcal{K}_c$.

When the parameter is $c \notin \mathcal{M}$, the critical orbit escapes to ∞ and $\mathcal{K}_c = \partial\mathcal{K}_c$ is a Cantor set. Equipotential lines are unions of Jordan curves or figure-8s, and pairs of dynamic rays crash into the critical point $z = 0$ or into precritical points; i.e., there are two arcs going in and two arcs going out. The Boettcher map $\Phi_c(z)$ is still defined in a neighborhood of $z = \infty$, which contains the critical value $z = c$; it turns out that the map $\Phi_{\scriptscriptstyle M}(c) = \Phi_c(c)$ is conformal $\widehat{\mathbb{C}} \setminus \mathcal{M} \to \widehat{\mathbb{C}} \setminus \overline{\mathbb{D}}$. External rays and equipotential lines are defined in the exterior of the Mandelbrot set as preimages of radial lines and circles under $\Phi_{\scriptscriptstyle M}(c)$; the former are called **parameter rays**.

When the angle is preperiodic under doubling, the ray lands at a **Misiurewicz point** $c \in \mathcal{M}$, for which the critical orbit is preperiodic. Now c is of β-**type**, if it is iterated to the fixed point β_c; then the angle is dyadic. Periodic rays land in pairs at **roots** of **hyperbolic components** Ω [29, 39], bounding a **wake**. For $c \in \Omega$ the critical orbit converges to an attracting cycle. When Ω is of **satellite** type, it bifurcates from some Ω'; otherwise it is **primitive**. In both cases, there is a unique root $c \in \partial\Omega$, where the attracting cycle becomes parabolic with multiplier 1. Satellite components and **sublimbs** are attached to $\partial\Omega$ at parabolic parameters with multiplier $\neq 1$. When two or more rays land at the same parameter $c \in \partial\mathcal{M}$, then $\mathcal{M} \setminus \{c\}$ is disconnected. All c' in a component not containing 0 are **behind** c.

2.2 Corresponding puzzle-pieces

External rays with rational angles can be used to cut the parameter plane or a dynamic plane into specified pieces; by restricting these to the interior of an equipotential line, bounded disks are obtained [36]. The landing points are called **vertices** of the parapuzzle-piece or puzzle-piece; a piece with one vertex is a **sector**, and a piece with two vertices is a **strip**. See the examples in Figure 4.

Proposition 2.1 (Puzzle-pieces and correspondence)
1. *For $c \in \mathbb{C}$, a **puzzle-piece** P_c is a disk bounded by the ends of finitely many dynamic rays at rational angles, which land together in pairs, and by subarcs of a single equipotential line. For $c \in \mathcal{M}$, both $\mathcal{K}_c \cap P_c$ and $\mathcal{K}_c \cap \overline{P_c}$ are connected.*

If $0 \notin P_c$, then $f_c : P_c \to f_c(P_c)$ is conformal; it is a branched cover, when $0 \in P_c$ and $P_c = -P_c$.

2. *A **parapuzzle-piece** $\mathcal{P}_{\scriptscriptstyle M}$ is a disk bounded by the ends of finitely many parameter rays at rational angles landing in pairs, and by subarcs of a single eqiupotential line. Now $\mathcal{M} \cap \mathcal{P}_{\scriptscriptstyle M}$ and $\mathcal{M} \cap \overline{P_{\scriptscriptstyle M}}$ are connected.*

3. *For a parapuzzle-piece $\mathcal{P}_{\scriptscriptstyle M}$, there are **corresponding** puzzle-pieces P_c, $c \in P_{\scriptscriptstyle M}$, if these are bounded by rays with the same angles as for $P_{\scriptscriptstyle M}$ landing in the same pattern. So $c \in P_c$ and the vertices do not bifurcate for $c \in P_{\scriptscriptstyle M}$, which means in particular that no vertex of P_c is iterated back to P_c.*

Conversely, given a parameter $c_* \in \mathbb{C}$ and a puzzle-piece P_* with $c_* \in P_*$ and such that no vertex is iterated back to $\overline{P_*}$, there is a corresponding parapuzzle-piece $P_{\scriptscriptstyle M}$ and a family of puzzle-pieces P_c, $c \in P_{\scriptscriptstyle M}$.

The latter statements are based on a stability result for landing patterns: periodic dynamic rays bifurcate only at certain roots, while preperiodic rays bifurcate also at Misiurewicz points where they are precritical [29, 39]. Note that when a vertex of P_c is iterated to another vertex, stability depends on the choice of branches of $\mathcal{K}_c$ included in P_c. See also Remark 2.4 for holomorphically moving pieces. Certain pieces may be constructed in an interplay between parameter plane and dynamic planes: when P_c correspond to P_M, all iterated preimages of P_c have angles independent of $c \in P_M$ as long as they do not intersect $f_c^{-1}(P_c)$; when they do, the landing pattern bifurcates at some parameter $c = a \in P_M$, which gives rise to a subdivision of P_M.

2.3 Quasiconformal maps and holomorphic motions

A K-**quasiconformal** map $\varphi : U \to V$ is a homeomorphism with specific regularity properties, which are well-adapted to several applications in complex dynamics; see [3, 14, 30] for various definitions and basic properties. The analytic definition may be given by comparing φ to a diffeomorphism: on the one hand, φ has the stronger property that its tangent maps send circles to ellipses with axes ratio bounded uniformly by K, and on the other hand, φ only needs to be weakly differentiable with distributional derivatives in L^2_{loc}.

When $U_M \subset \mathbb{C}$ is a disk and $X \subset \mathbb{C}$, a **holomorphic motion** of X over U_M is a map $U_M \times X \to \mathbb{C}$, $(c,\, z) \mapsto i_c(z)$, such that $z \mapsto i_c(z)$ is injective on X for $c \in U_M$ and $c \mapsto i_c(z)$ is holomorphic on U_M for $z \in X$. We shall write $i_c : X \to \mathbb{C}$, $c \in U_M$. Fundamental properties of holomorphic motions are due to Lyubich, Mañé–Sad–Sullivan, and Słodkowsky [27, 42, 1, 14]:

Theorem 2.2 (Słodkowsky extension and λ-Lemma)
For any subset $X \subset \mathbb{C}$, a holomorphic motion $i_c : X \to \mathbb{C}$, $c \in U_M$, extends to a holomorphic motion of $\mathbb{C}$ over U_M.

$i_c : \mathbb{C} \to \mathbb{C}$ is quasiconformal; when there is a base point $c_* \in U_M$ with $i_* = \mathrm{id}$, the dilatation $K(c)$ is bounded in terms of the hyperbolic distance of c to c_* in U_M.

The following result is the main technical tool for constructing embedded Julia sets, and it is useful for local connectivity [36] and in renormalization as well:

Proposition 2.3 (Holonomy is quasiconformal, following Lyubich)
*Suppose $U_M \subset \mathbb{C}$ is a Jordan disk and for c in a neighborhood $\widetilde{U}_M \supset \overline{U_M}$, $i_c : \mathbb{C} \to \mathbb{C}$ is a holomorphic motion with base point $c_* \in U_M$. For a holomorphic $f : \widetilde{U}_M \to \mathbb{C}$ define the **holonomy** map $h : \widetilde{U}_M \to \mathbb{C}$ with $h(c) = i_c^{-1}(f(c))$. Assume that there is a Jordan disk U_*, such that $h : \partial U_M \to \partial U_*$ is an orientation-preserving homeomorphism. Then $h : U_M \to U_*$ is quasiconformal.*

In the special case of a smooth holomorphic motion, quasiconformality of h is due to [5]. The general case, which is needed in the present paper, was obtained by Lyubich [25, 26], using similar techniques as Shishikura [41]. See also Appendix B for the **proof** and for an example showing that $\widetilde{U}_M \supset \overline{U_M}$ is needed: otherwise not only quasiconformality breaks down, but $h(U_M)$ may be a proper subset of the expected U_*.

Remark 2.4 (Holomorphic motion of puzzle-pieces)
1. Proposition 2.3 applies to puzzle-pieces in particular, where $U_c = i_c(U_*)$ correspond to U_M. Uusually we have $i_c = \Phi_c^{-1} \circ \Phi_*$ on ∂U_* and $h = \Phi_*^{-1} \circ \Phi_M$ on ∂U_M. Note that stability on $\widetilde{U}_M \supset \overline{U_M}$ means that all vertices of U_c are preperiodic and none is iterated back to $\overline{U_c}$.

2. Dynamic rays landing at a repelling periodic or preperiodic point spiral according to the multiplier; the asymptotic geometry can be changed by a quasiconformal *map but not by a smooth map. So in general a puzzle-piece is a quasidisk and its boundary is not piecewise smooth. For the same reason, the holomorphic motion of a puzzle-piece or of a Julia set is not smooth.*

2.4 Primitive and satellite renormalization

A suitable restriction $g_c(z)$ of $f_c^p(z)$ is a **renormalization**; it is related to another quadratic polynomial by **straightening**. A holomorphic map $g : U' \to U$ is called **quadratic-like**, if the disks satisfy $\overline{U'} \subset U$ and $g(z)$ is proper of degree 2. Then $g(z)$ is **hybrid-equivalent** to some $f_{\widehat{c}}(\widehat{z})$, i.e., there is a quasiconformal $\psi(z)$ with $\psi \circ g = f_{\widehat{c}} \circ \psi$ and ψ is complex differentiable a.e. on the **small Julia set**, the filled Julia set of $g(z)$. Here ψ is defined on all of U when the disks are quasidisks.

The construction of ψ need not be discussed here, but it starts with a quasiconformal map $\xi : \overline{U} \setminus U' \to \overline{\mathbb{D}_{R^2}} \setminus \mathbb{D}_R$ satisfying $\xi \circ g = F \circ \xi$ on $\partial U'$, with $F(z) = z^2$. Then $\Phi_{\widehat{c}} \circ \psi = \xi$ on the fundamental annulus. If the critical orbit of g escapes, an appropriate extension of $\xi(z)$ maps the critical value to $\Phi_{M}^{-1}(\widehat{c})$. On the other hand, when the small Julia set is connected, $\widehat{c}$ is independent of $R > 1$ and $\xi(z)$.

Theorem 2.5 (Douady–Hubbard renormalization)
1. *For any hyperbolic component $\Omega \subset \mathcal{M}$ of period $p \ge 2$, there is a* ***small Mandelbrot set*** *$\mathcal{M}_p \subset \mathcal{M}$ with $\partial\mathcal{M}_p \subset \partial\mathcal{M}$ and a straightening homeomorphism χ_ξ with $\chi_\xi : \mathcal{M}_p \to \mathcal{M}$, which maps Ω to the main cardioid.*

a) When Ω is primitive, there are holomorphically moving puzzle-pieces with $f_c^p : U_c' \to U_c$, such that the only vertex of U_c is preperiodic and not iterated back to $\overline{U_c}$. Choose $\xi_c = \xi_* \circ i_c^{-1}$ for a suitable holomorphic motion with base point $c_* = c_p$ and define $\widehat{c} = \chi_\xi(c)$ by straightening f_c^p, then χ_ξ is quasiconformal on U_M.

b) When Ω is a satellite component, there is a similar construction within every subwake, such that the vertices of U_c are iterated back to $\overline{U_c}$ but only close to the small β; in the exterior of $\mathcal{M}_p$ the homeomorphism $\chi(c)$ is locally quasiconformal in subwakes. Only the root of $\mathcal{M}_p$ is not p-renormalizable.

Conversely, every simply p-renormalizable parameter $c \in \mathcal{M}$ belongs to a small Mandelbrot set $\mathcal{M}_p$; it is obtained by ***tuning*** *$\widehat{c}$.*

2. *When $\mathcal{M}_p$ is primitive, its* ***decorations*** *are the connected components of $\mathcal{M} \setminus \mathcal{M}_p$. They are attached at tuned β-type Misiurewicz points and labeled by dyadic angles. If $\mathcal{M}_p$ is a satellite Mandelbrot set of a component of period $q = p/r$, each decoration has $r - 1$ components.*

The concise notation $\mathcal{M}_p$ must be supplemented with parameters or external angles, when the context does not specify $\mathcal{M}_p$ uniquely. The **proof** is spread over several sources [5, 11, 25, 40] and a comprehensive presentation will be given in [18], including unpublished folk results concerning the locus of renormalization, the Douady substitution [6] for irrational angles, and bifurcations of decorations.

The classical construction from [5, 29] starts with a puzzle-piece thickened at its two points of intersection with $\mathcal{K}_c^p$, which moves only continuously with c. Restricting to smaller domains moving smoothly, it is shown that $\chi(c)$ is continuous on $\mathcal{M}_p$, and that its restriction to $\mathcal{M}_p$ has a mapping degree in a generalized sense. In the primitive case, Haïssinsky [11] constructed puzzle-pieces U_c', U_c with preperiodic angles and extended the holomorphic motion with the Słodkowsky Theorem 2.2, but he referred to [5] for the proof that χ is a homeomorphism on $\mathcal{M}_p$, and he did not consider parameters $c \in U_{\scriptscriptstyle M} \setminus \mathcal{M}_p$. — In my opinion, there are several advantages when puzzle-pieces moving holomorphically are used from the start:

- The same motion is used throughout, and there is no need to restrict domains.
- The concept of mapping degree is needed only on an open disk.
- It is straightforward to control the image of decorations under χ_ξ, which gives landing properties of irrational rays at $\partial\mathcal{M}_p$.
- For $U_c^n = f_c^{-np}(U_c)$ the bounded number of intersections $\partial U_c^n \cap \mathcal{M}$ allows a geometric description of segments on decorations, which can be used to give a simplified proof of the Shrinking Decorations Theorem [9, 34].

Unfortunately, the Słodkowsky Theorem 2.2 was not yet available when [5] was written. Since the proof is rather involved, modern textbooks and courses may try to avoid it as well [26], but it is needed in any case for the construction of embedded Julia sets, since the holomorphic motion of small Julia sets is not smooth. — See Appendix B for the construction and bifurcations of decorations and carrots.

3 Embedded Julia sets

Embedded Julia sets of the first level are constructed in Sections 3.1 and 3.2, while higher levels and the geometry of $\mathcal{K}_{\scriptscriptstyle M}^{1\cdot m,\,p} \subset \mathcal{M}$ are discussed in Sections 3.3 and 3.4.

3.1 General analytic construction

The following Proposition 3.1 gives a fairly general construction of embedded Julia sets, where puzzle-pieces are mapped $f_c^m : V_c \to U_c$, U_c contains the disconnected small Julia set $\mathcal{K}_c^p$, and V_c contains the preimage corresponding to the embedded Julia set $\mathcal{K}_{\scriptscriptstyle M}^{m,\,p}$ in the parameter plane. See Figure 4. The same techniques apply to arbitrary Jordan domains, and they are implicit in [8, 21]; as discussed in the Introduction, corresponding puzzle-pieces are easily constructed combinatorially, while disks corresponding to round disks are found from approximate expressions for iterates of $f_c(z)$, which are related to Misiurewicz points or to parabolic parameters.

Proposition 3.1 (General construction of embedded Julia sets)
Suppose $\mathcal{M}_p$ is a small Mandelbrot set of period p and $W_{\scriptscriptstyle M}$ is the wake of $\mathcal{M}_p$ if $\mathcal{M}_p$ is of satellite type, or $W_{\scriptscriptstyle M}$ is the wake of a suitable Misiurewicz point according to Theorem 2.5 if $\mathcal{M}_p$ is primitive. Consider a parapuzzle-piece $\overline{V_{\scriptscriptstyle M}} \subset W_{\scriptscriptstyle M} \setminus \mathcal{M}_p$, such that for c in a neighborhood of $\overline{V_{\scriptscriptstyle M}}$ we have holomorphically moving puzzle-pieces U_c, U'_c, V_c with $\overline{U'_c} \subset U_c$ and $\overline{V_c} \subset U_c$, where V_c corresponds to $V_{\scriptscriptstyle M}$, and such that $f_c^p : U'_c \to U_c$ and $f_c^m : V_c \to U_c$ are proper of degree 2 for some m. Then:

1. *The small Julia set $\mathcal{K}_c^p$ is defined for $c \in W_{\scriptscriptstyle M}$; it is connected for $c \in \mathcal{M}_p$ and a Cantor set otherwise. We shall assume that it agrees with the filled Julia set of $f_c^p : U'_c \to U_c$. Now $\mathcal{K}_c^p$ moves holomorphically for c in a neighborhood of $\overline{V_{\scriptscriptstyle M}}$.*
2. *For c in a neighborhood of $\overline{V_{\scriptscriptstyle M}}$ define $\mathcal{K}_c^{m,\,p} := \{z \in V_c \,|\, f_c^m(z) \in \mathcal{K}_c^p\} \subset \partial\mathcal{K}_c$. This set is a conformal image of $\mathcal{K}_c^p$ and moves holomorphically as well.*

3. *An* ***embedded Julia set*** *is defined as* $\mathcal{K}_M^{m,p} := \{c \in V_M \,|\, c \in \mathcal{K}_c^{m,p}\}$. *It is a Cantor set in* $\partial\mathcal{M}$ *and a quasiconformal image of* $\mathcal{K}_c^{m,p}$ *and* $\mathcal{K}_c^p$ *for any* $c \in V_M$.

The notation $\mathcal{K}_M^{m,p}$ is somewhat generic, since there will be several embedded Julia sets for suitable m and p, and we need to give parameters or external angles to specify one uniquely. Note that in general we do not have a holomorphic motion of puzzle-pieces for c in a domain U_M corresponding to U_c: V_c may be bifurcating, and in the satellite case, U_c is constructed separately in the subwakes of $\mathcal{M}_p$.

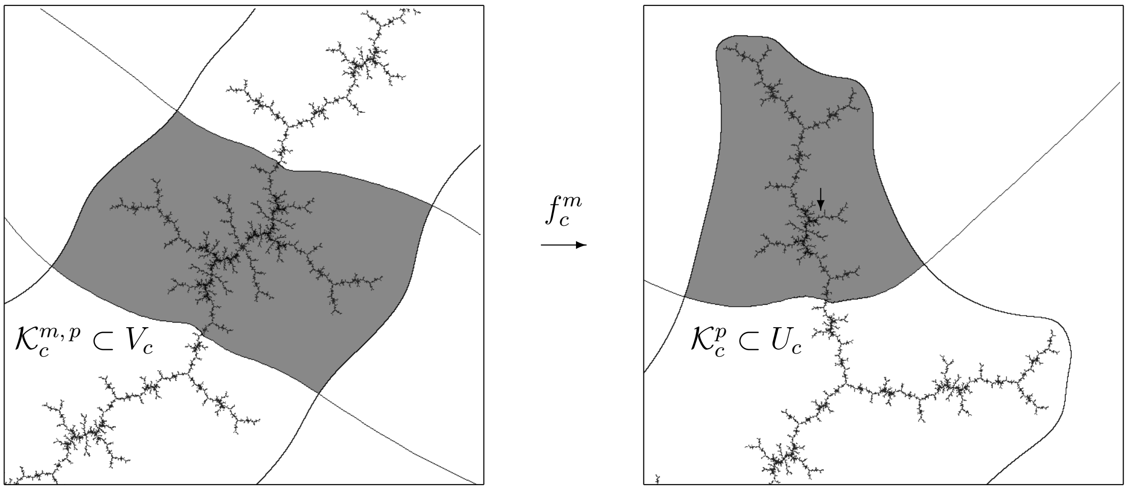

Figure 4: The 1/4-decoration of the small Mandelbrot set $\mathcal{M}_4$ contains an embedded Julia set $\mathcal{K}_M^{23,4} \subset \partial\mathcal{M}$, such that the tiny Mandelbrot set $\mathcal{M}_{23}$ has the external angles 1679906/8388607 and 1710489/8388607 at its root; denote the center by $c = c_{23}$.
Left: $\mathcal{K}_c^{23,4} = \mathcal{K}_c^{1\cdot 23,4} \subset \partial\mathcal{K}_c$ and the domain $V_c \subset U_c$ with $f_c^{23} : V_c \to U_c$.
Right: the small Julia set $\mathcal{K}_c^4 \subset U_c$ is the 2-to-1 image of $\mathcal{K}_c^{23,4}$ under f_c^{23}. The arrow marks the location of $V_c \subset U_c$, which is not visible on this scale.
The corresponding embedded Julia set $\mathcal{K}_M^{23,4} \subset \partial\mathcal{M}$ is shown in Figures 8, 9, and 12.

Proof: 1. For c in a neighborhood of $\overline{V_M}$, the small Julia set $\mathcal{K}_c^p = \partial\mathcal{K}_c^p \subset \partial\mathcal{K}_c$ is the closure of its repelling periodic points. These bifurcate only at roots, where they become parabolic, and they are interchanged when c moves on a closed curve around such a root. But V_M is simply connected and does not contain any of these roots c, since $\mathcal{K}_c^p$ would be connected if it contained a parabolic point, and $c \in \mathcal{M}_p$. So a dense subset of $\mathcal{K}_c^p$ moves holomorphically, and this motion extends uniquely to all of $\mathcal{K}_c^p$ by the λ-Lemma or the Słodkowsky Theorem 2.2. — Note that U_c need not be the puzzle-piece used in the definition of $\mathcal{M}_p$ and we may use different puzzle-pieces for different embedded Julia sets at the same small $\mathcal{M}_p$.

2. Now $f_c^m : \mathcal{K}_c^{m,p} \to \mathcal{K}_c^p$ is 2-to-1, but $f_c^{m-1} : \mathcal{K}_c^{m,p} \to f_c^{-1}(\mathcal{K}_c^p)$ is conformal on V_c , and $f_c^{p-1} : \mathcal{K}_c^p \to f_c^{-1}(\mathcal{K}_c^p)$ is conformal on U_c' .

3. The boundary ∂V_c moves holomorphically by a composition of Boettcher maps and $\mathcal{K}_c^{m,p}$ moves holomorphically according to item 2. For any base point $c_* \in V_M$, the Słodkowsky Theorem 2.2 provides an extension $i_c : \mathbb{C} \to \mathbb{C}$ for c in a neighborhood of $\overline{V_M}$. The holonomy $h : V_M \to V_*$ with $h(c) = i_c^{-1}(c)$ is quasiconformal according to Proposition 2.3, since the rays and equipotential lines in ∂V_c correspond to those in ∂V_M . Now

$$c \in \mathcal{K}_M^{m,p} \;\Leftrightarrow\; c \in \mathcal{K}_c^{m,p} \;\Leftrightarrow\; c \in i_c(\mathcal{K}_*^{m,p}) \;\Leftrightarrow\; h(c) \in \mathcal{K}_*^{m,p} \tag{1}$$

shows that $\mathcal{K}_M^{m,p} = h^{-1}(\mathcal{K}_*^{m,p})$, and $* = c_* \in V_M$ was arbitrary. Finally, $\mathcal{K}_M^{m,p}$ is the closure of a countable family of Misiurewicz points, which correspond to preperiodic points in $\mathcal{K}_c^{m,p}$ and to periodic points in $\mathcal{K}_c^p$, thus $\mathcal{K}_M^{m,p} \subset \partial\mathcal{M}$. ∎

So quasiconformality is obtained from the holonomy $h(c) = i_c^{-1}(c)$ according to Proposition 2.3 and Remark 2.4.1, which satisfies $h(\mathcal{K}_M^{m,p}) = \mathcal{K}_*^{m,p}$: it describes the parameters c, such that the moving Cantor set $\mathcal{K}_c^{m,p}$ meets the critical value c. This is visualized nicely in Figure 13 of [2] and Figure 7 of [21]. The holonomy map h was constructed by Lyubich [25] to show that the straightening map $\chi : \mathcal{M}_p \to \mathcal{M}$ is quasiconformal; it does not appear explicitly in [8], however, because their proof is formulated with χ instead. — Note that all quadratic Cantor Julia sets are quasiconformally homeomorphic, so the statement relating $\mathcal{K}_M^{m,p}$ and $\mathcal{K}_c^p$ is rather weak without a bound on the dilatation. Actually, the dilatation of i_c and h is bounded in terms of the diameter of $\mathcal{K}_M^{m,p}$ divided by its distance to $\partial\mathcal{M}_p$, since this quantity estimates the hyperbolic diameter of $\mathcal{K}_M^{m,p}$ within a disk where the motion is holomorphic.

Remark 3.2 (Embedded Julia set surrounds a tiny Mandelbrot set)
For $c \in V_M$, $f_c^m : V_c \to U_c$ gives a quadratic-like family $f_c^m : V_c' \to V_c$ and defines a primitive small Mandelbrot set $\mathcal{M}_m \subset V_M$, which shall be called the tiny Mandelbrot set associated to the embedded Julia set $\mathcal{K}_M^{m,p}$. This notion is not needed to define $\mathcal{K}_M^{m,p} = \mathcal{K}_M^{1\cdot m,p}$, but it will be useful in Section 3.3 to construct embedded Julia sets $\mathcal{K}_M^{l\cdot m,p}$ of higher levels $l \ge 2$.

It remains to construct examples of puzzle-pieces satisfying the assumptions of Proposition 3.1. In the following Section 3.2 we shall see combinatorially, that for every $\mathcal{M}_p$ there are embedded Julia sets dense at $\partial\mathcal{M}_p$. Consider the converse question: given $\mathcal{M}_p$ and $\mathcal{M}_m$, is there an associated $\mathcal{K}_M^{m,p}$? We must choose V_c small enough such that f_c^{m-1} is injective on V_c, and V_c must be big enough so that $f_c^{m-1}(V_c)$ contains $f_c^{-1}(\mathcal{K}_c^p)$. This is not always possible; see Figure 7, Example 3.9, and Remark 3.14.2. On the other hand, when a primitive $\mathcal{M}_m \subset W_M$ is before $\mathcal{M}_p$, then $\mathcal{K}_M^{m,p}$ always exists.

3.2 Combinatorial construction

Given a small Mandelbrot set $\mathcal{M}_p$, embedded Julia sets $\mathcal{K}_M^{m,p}$ are obtained by constructing suitable puzzle-pieces combinatorially, which satisfy the assumptions of Proposition 3.1. Items 1 and 2 are shown by analytic methods in [21]; the case of a primitive root is due to [8].

Theorem 3.3 (Embedded Julia sets at a small Mandelbrot set)
Suppose $\mathcal{M}_p \subset \mathcal{M}$ is a primitive or satellite small Mandelbrot set of period p.

1. *For any parabolic parameter or Misiurewicz point $a \in \partial\mathcal{M}_p$ there is a sequence of embedded Julia sets $\mathcal{K}_M^{m_j,p} \subset \partial\mathcal{M}$ with $\mathcal{K}_M^{m_j,p} \to \{a\}$ in the Hausdorff metric. Here m_j increases by the period of a.*

2. *For any $b \in \partial\mathcal{M}_p$ there is a sequence of embedded Julia sets $\mathcal{K}_M^{m_j,p} \subset \partial\mathcal{M}$ with $\mathcal{K}_M^{m_j,p} \to \{b\}$ as $j \to \infty$.*

3. *When b is not parabolic, this sequence can be chosen such that there are affine maps A_j and $A_j(\mathcal{K}_M^{m_j,p})$ converges to a conformal copy of the small Julia set $\mathcal{K}_b^p$, which is a quasiconformal copy of $\mathcal{K}_{\widehat{b}}$.*

When $\mathcal{M}_p$ is primitive, choose $U_c\,, U_c'$ such that U_c corresponds to a parapuzzle-piece with one vertex; in the satellite case, we may choose U_c with one vertex in each component of the $0/1$-decoration, but this is done with separate constructions in each sublimb of $\mathcal{M}_p$. Now the basic aim is to find puzzle-pieces V_c, which are mapped injectively to $f_c^{-1}(U_c)$ by some f_c^{m-1}. We shall consider two different strategies in fact: the first one is simpler and it does not require a distinction between different cases, while the second one is adapted to renormalization, which will be useful in Section 3.4. Moreover, the second one immediately gives sequences of embedded Julia sets converging to boundary points of $\mathcal{M}_p$ where decorations are attached, while the first one gives sequences converging to tips of decorations, and we need to consider sufficiently small decorations.

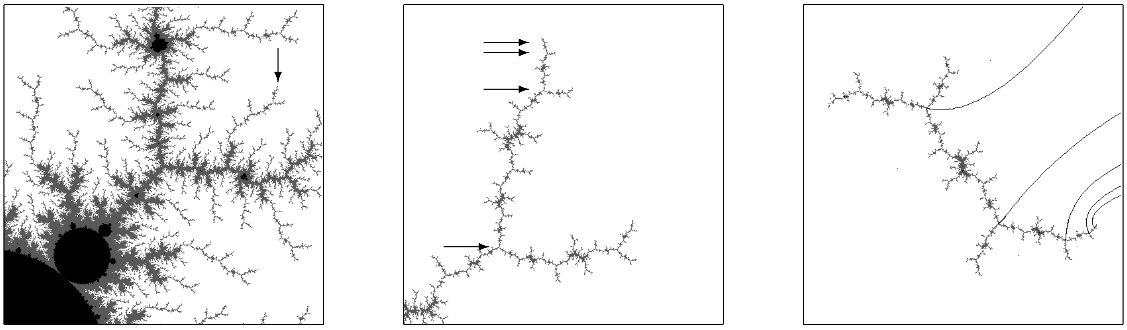

Figure 5: Left: a subset of $\mathcal{M}$ around a Misiurewicz point $a \in \mathcal{M}_4$, which is obtained by tuning the Misiurewicz point with angle $9/56$ in the $1/3$-limb.
Middle: zoom to the β-type Misiurewicz point marked in the left image. The arrows indicate vertices of adjacent parameter edges. These are used to construct embedded Julia sets in the first proof of Theorem 3.3.1.
Right: adjacent dynamic edges converging to β_a, marked by dynamic rays.

Proof of item 1 using edges: A dynamic edge of order m is a subset of $\mathcal{K}_c$ with two vertices, which is mapped injectively to the subset between the fixed point α_c and $-\alpha_c$ by f_c^{m-1}; a parameter edge is a subset of $\mathcal{M}$ corresponding to dynamic edges [16, 17]. There is a sequence of dynamic edges converging to the other fixed point β_c, there are preimage edges at every preimage of β_c, and for every β-type Misiurewicz point there is a corresponding sequence of adjacent parameter edges. See Figure 5. Now β-type Misiurewicz points are dense in $\partial\mathcal{M}$, so we find a parameter edge within any neighborhood of $a \in \partial\mathcal{M}_p$. Since f_c^{m-1} maps the corresponding dynamic edge to the central edge containing $f_c^{-1}(\mathcal{K}_c^p)$, we can define V_c and $V_{\scriptscriptstyle M}$ such that $f_c^{m-1}(V_c) = f_c^{-1}(U_c)$. Note that ∂U_c is not iterated back to U_c in the primitive case, and not to the part containing c in the satellite case when U_c is small, so V_c moves holomorphically. Finally, to construct a sequence m_j increasing by the period when a is a parabolic parameter, choose one edge of appropriate order in each $1/j$-sublimb of the hyperbolic component with root a. When a is a Misiurewicz point, start with a preimage of $\beta_a \in \mathcal{K}_a$ close to a postcritical periodic point and pull it back towards this point. Since $\mathcal{M}$ is locally connected at $c = a$, or more precisely, the fiber of a is trivial [40], we have $\overline{V_{\scriptscriptstyle M}} \to \{a\}$ as $j \to \infty$.

Proof of item 1 using segments from renormalization: This strategy works best when a is a tuned β-type Misiurewicz point; recall from Theorem 2.5 that these are the points where a decoration is attached.

Case 1: $\mathcal{M}_p$ is primitive and a is its root or a tuned β-type Misiurewicz point. — For $c \in \mathcal{M}_p$, each dynamic decoration of $\mathcal{K}_c^p$ is cut into segments by the curves ∂U_c^n with $f_c^p : U_c^{n+1} \to U_c^n$ and $U_c^0 = U_c$. When c is in a parameter decoration, the corresponding dynamic decoration still exists, but its preimages have merged in pairs. This is not true for the 0/1-decoration: the segment containing $z = c$ exists but its preimages in the 0/1- and 1/2-decorations have merged. Corresponding segments of parameter decorations are marked with strips in Figure 6. Now a dynamic strip containing the critical value c is iterated injectively until it meets the 1/2-decoration, and if the parameter c was chosen close enough to $\partial\mathcal{M}_p$, it is iterated p more steps to the 0/1-decoration; after some more steps, it will become the strip with one vertex on $\partial U_c'$ and one on ∂U_c. Since strips are iterated injectively unless they contain $z = 0$, and since this cannot happen forever, there is an m such f_c^{m-1} maps our original strip to a strip around 0. Its vertices are iterates of $\partial U_c' \cap \mathcal{K}_c$, so they cannot be iterated to $\overline{U_c}$, and the strip contains $f_c^{-1}(\overline{U_c})$. Define V_c in the original strip such that f_c^{m-1} maps it to $f_c^{-1}(U_c)$, then it moves holomorphically for c in a neighborhood of the corresponding V_M. Again by triviality of the fiber, V_M can be constructed in any neighborhood of a, and taking the adjacent segment increases m by p. — Note that infinitely many embedded Julia sets can be obtained within a single segment in fact: the iterated strip around 0 consists of $f_c^{m-1}(V_c) = f_c^{-1}(U_c)$ and two complementary pieces, which can be iterated further.

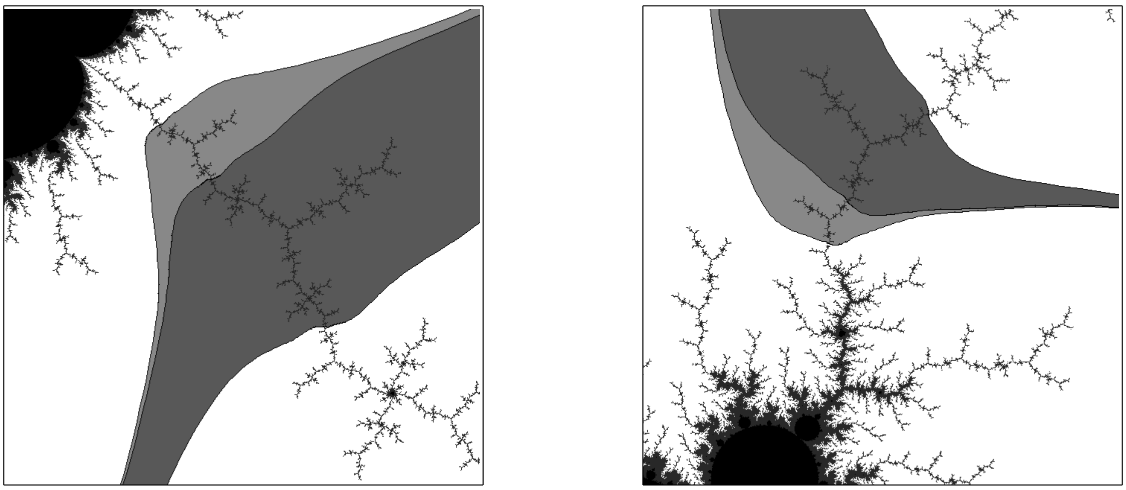

Figure 6: In the 0/1- and 1/4-decorations of the primitive small Mandelbrot set $\mathcal{M}_4$, two segments are marked with strips bounded by external rays. In each decoration there is a sequence of adjacent segments converging to the root of $\mathcal{M}_4$ or to the tuned β-type Misiurewicz point, respectively. Here U_c is defined by the angles 199/1008 and 269/1008, the same as in Figure 1; their preimages define the segments. These are used to construct embedded Julia sets in the second proof of Theorem 3.3.1, case 1.

Case 2: $\mathcal{M}_p$ is satellite and a is a tuned β-type Misiurewicz point. — Here the same approach would not work, because the segments may be iterated to a subset of $f_c^{-1}(U_c)$. First, let us look at the dynamics for c in the main hyperbolic component of period p; see the example of the Basilica in Figure 7 left. The biggest Fatou component in this image is attached to $\mathcal{K}_c^2$ at internal angle 1/4 and we may ask whether this component, and the components attached to it directly or indirectly, correspond to embedded Julia sets in the 1/4-decoration of $\mathcal{M}_2$. This is not always true: for that component itself it is explained in the figure. For the components attached to it at internal angles $+1/2^n$, $n \ge 3$, e.g., there is pairwise merging of preimages of 1/4; the remaining components, e.g., with angles $-1/2^n$, $n \ge 2$, do not bifurcate. This means that the strip containing such a component corresponds to a strip in the parameter plane, and when c is within these strips, the dynamic strip is iterated injectively to a strip containing $f_c^{-1}(K_c^2)$ in its closure. Now choose slightly larger strips bounded by preimages of the $2 \cdot 3$-cycle to define V_c and U_c, respectively, and apply Proposition 3.1.

Again, choosing subsequent values of j for the internal angles $-1/2^j$ gives embedded Julia sets with preperiod m growing by $p = 2$, and converging to the tuned β-type Misiurewicz point a. Note that in contrast to the primitive case, we may need to shrink U_c as j and m are increased. — The same construction works for all sublimbs of $\mathcal{M}_2$ and for all small satellite Julia sets of periods $p \ge 2$, except in the respective 1/2-sublimb: then all strips around components attached at internal angle $\pm 1/2^n$ bifurcate, as the parameter c moves from $\mathcal{M}_p$ into this sublimb. In this case, the analogous construction works with components attached indirectly.

Case 3: a is any other parabolic parameter or Misiurewicz point in $\partial\mathcal{M}_p$. — Then approximate it with tuned β-type Misiurewicz points und use the result of case 1 or 2, respectively.

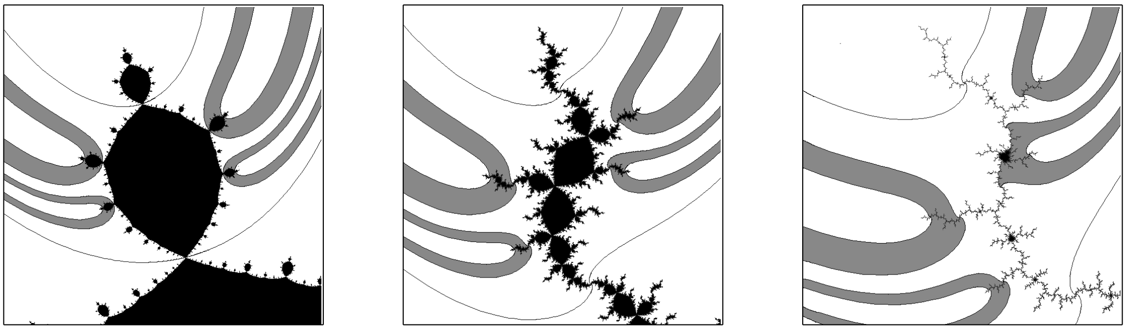

Figure 7: Consider an example of case 2 in the second proof of Theorem 3.3.1. Here a is the tuned β-type Misiurewicz point, where the 1/4-decoration is attached to the tuned 1/3-limb within the 1/3-sublimb. The central component in the left image is mapped to $\mathcal{K}_*^2$ in $m = 5$ iterations and there is a corresponding tiny Mandelbrot set $\mathcal{M}_5$, but there is no embedded Julia set $\mathcal{K}_M^{5,2}$: it would be directly attached to $\mathcal{M}_2$, cf. Remark 3.2. (It could be defined by a piecewise construction, losing quasiconformality.)
The gray strips have the same angles in the three images; in the left image, they mark components attached at internal angles $\pm 1/4$ and $\pm 1/8$ to the larger component at internal angle 1/4. Note that in the right image, the strip with angle 1/8 has bifurcated, because 1/8 is mapped to 1/4 under doubling. The middle image suggest that strips can be enlarged by choosing vertices with period $2 \cdot 3$ and high preperiod.

Proof of items 2 and 3: Suppose $a \in W_M$ is a β-type Misiurewicz point. For c in a neighborhood of a there is a Königs conjugation φ_c with $\varphi_c(f_c(z)) = \rho_c \cdot \varphi_c(z)$, normalized as $\varphi_c'(\beta_c) = 1$. Here the repelling multiplier is $\rho_c = f_c'(\beta_c)$ and φ_c is defined in a neighborhood of β_c bounded by dynamic rays at the other fixed point α_c. Now choose k such that a small neighborhood of $z = a$ is mapped conformally onto the domain of φ_a by f_a^k; in general k will be larger than the preperiod. Then for $n \ge 0$ there are stable dynamic edges, parameter edges, and embedded Julia sets of order $m = m_n = k + n + 1$ converging to $c = a$. See the example in Figure 5, and Section 4.2 for a more detailed explanation. So

$$c \in \mathcal{K}_M^{m,\,p} \ \Leftrightarrow\ c \in \mathcal{K}_c^{m,\,p} \ \Leftrightarrow\ \rho_c^n \cdot \varphi_c(f_c^k(c)) \in \varphi_c(f_c^{-1}(\mathcal{K}_c^p)) \ . \tag{2}$$

Now the set on the right hand side moves holomorphically and converges as $c \to a$; on the left hand side we have $\rho_c^n = \rho_a^n \cdot (1 + \mathcal{O}(n\rho_a^{-n}))$ and $\varphi_c(f_c^k(c))$ has a linear approximation for $c \approx a$. This gives

$$\rho_a^n \cdot \Big(\frac{d}{dc}\,\varphi_c(f_c^k(c))\Big|_{c=a}\Big) \cdot \Big(\mathcal{K}_M^{m,\,p} - c_m\Big) \ \to\ \varphi_a(f_a^{-1}(\mathcal{K}_a^p)) - \varphi_a(0) \tag{3}$$

as $m = k + n + 1 \to \infty$. Here c_m is the center of period m in the parameter edge of order m. Given any $b \in \partial\mathcal{M}_p$, we may approximate it with β-type Misiurewicz points a_j and choose k_j and n_j appropriately; when b is not parabolic, continuity of small Julia sets according to Proposition B.2 gives $\varphi_a(f_a^{-1}(\mathcal{K}_a^p)) \to \varphi_b(f_b^{-1}(\mathcal{K}_b^p))$.

The same idea works when $a_j \in \partial\mathcal{M}_p$ are tuned β-type Misiurewicz points, with two changes: since $z = 0$ need not be in the domain of φ_c, we use $f_c^{-l}(\mathcal{K}_c^p)$ for some $l \ge 1$. And the period is p now, so $m = k + np + l$. Here only $k = k_j$ and $n = n_j$ depend on j while l stays the same; therefore $\varphi_a(f_a^{-l}(\mathcal{K}_a^p)) \to \varphi_b(f_b^{-l}(\mathcal{K}_b^p))$. ■

See the examples in Figure 8 top. Note that this proof only uses the most basic techniques of asymptotic dynamics at Misiurewicz points [5, 43]. Estimates for f_c^m, $c \approx c_m$, are used only for the similarity phenomena in Sections 4.3 and 4.4, and not to obtain embedded Julia sets according to Theorems 3.3 and 3.6.

Remark 3.4 (Parabolic parameters and Siegel parameters)
When $b \in \partial\mathcal{M}_p$ is a parabolic parameter, for a sequence $c_j \to b$ there may be a limit set $\mathcal{K}_{c_j}^p \to \mathcal{L}$ with strict inclusions $\partial\mathcal{K}_b^p \subset \mathcal{L} \subset \mathcal{K}_b^p$. This phenomenon is called parabolic implosion. The limit set depends on the sequence, and it is not known, whether affine rescalings of $\mathcal{K}_M^{m_j,\,p}$ may converge to a limit set.

The case of a Siegel parameter $b \in \partial\mathcal{M}_p$ in Theorem 3.3.3 is interesting, because here $\mathcal{K}_M^{m,\,p} \subset \partial\mathcal{M}$ is a Cantor set, whose affine image approximates a small filled Julia set with non-empty interior. See the example in Figure 2 right. It is not known, whether the Hausdorff dimension of these Cantor sets converges to 2.

The analytic construction of $\mathcal{K}_M^{m,\,p}$ is summarized in the following diagram, where $c \in V_M$ is the base point of the holomorphic motion and h is the holonomy map:

$$\mathcal{K}_{\widehat{c}} \xleftarrow{\ \psi_c\ } \mathcal{K}_c^p \xrightarrow{\ f_c^{p-1}\ } f_c^{-1}(\mathcal{K}_c^p) \xleftarrow{\ f_c^{m-1}\ } \mathcal{K}_c^{m,\,p} \xleftarrow{\ h\ } \mathcal{K}_M^{m,\,p} \ . \tag{4}$$

The two arrows in the middle are conformal maps, so the dilatation bound for $\mathcal{K}_{\widehat{c}} \to \mathcal{K}_M^{m,\,p}$ depends on the straightening map and on the holomorphic motion. The latter bound is small when $\mathcal{K}_M^{m,\,p}$ has small hyperbolic diameter in V_M, in particular when its Euclidean diameter is much smaller than its distance to $\partial\mathcal{M}_p$.

Remark 3.5 (Kawahira–Kisaka)
In the present paper, embedded Julia sets $\mathcal{K}_M^{m,\,p}$ are considered to describe the local geometry of $\partial\mathcal{M}$ around a small Mandelbrot set $\mathcal{M}_p$, which reflects the geometry of the corresponding small Julia sets. Another interpretation is given by Tomoki Kawahira and Masahi Kisaka in Theorem C of [21]: small Julia sets of Misiurewicz

shape or imploded parabolic shape are dense everywhere at $\partial\mathcal{M}$. I.e., given a small disk $\mathcal{N}$ intersecting $\partial\mathcal{M}$ and $\widehat{b}$ close to $\partial\mathcal{M}$, there is an embedded Julia set $\mathcal{K}_M^{m,p} \subset \mathcal{N}$, such that a quasiconformal map from $\mathcal{K}_{\widehat{c}}$ to $\mathcal{K}_M^{m,p}$ has small dilatation and $\widehat{c}$ is close to $\widehat{b}$. Here a small Mandelbrot set $\mathcal{M}_p \subset \mathcal{N}$ is chosen first from a sequence converging to a Misiurewicz point, making the dilatation bound of the hybrid-equivalence ψ_c in (4) small. Then c_m is obtained, e.g., from a sequence of Misiurewicz points $a_j \to b \in \partial\mathcal{M}_p$; these sequences may be chosen such that the distance from $\mathcal{M}_p$ is much larger than the size of $\mathcal{K}_M^{m,p}$ to control the dilatation of h in (4).

By choosing $\widehat{b}$ such that the Hausdorff dimension of $\partial\mathcal{K}_{\widehat{b}}$ is almost 2, Kawahira–Kisaka obtain a modified proof that $\partial\mathcal{M}$ has Hausdorff dimension 2; in the original proof by Mitsuhiro Shishikura [41], only hyperbolic subsets of Julia sets are embedded into $\partial\mathcal{M}$. In addition, they remark that embedded Julia sets consist of semi-hyperbolic parameters, i.e., the critical point is not recurrent.

Parameter rays show a dimension paradox, which is slightly weaker than the known result for transcendental maps according to Bogusława Karpińska [22]: for any renormalization period $p \ge 2$ there is a set of angles with Hausdorff dimension $\le 1/p$, and a union of parameter rays with Hausdorff dimension $\le 1 + \frac{1}{p} < 2$, such that the landing points in $\partial\mathcal{M}$ form a set of Hausdorff dimension 2. To this end, either the construction of embedded Julia sets $\mathcal{K}_M^{m,p}$ above can be used, or the original construction by Shishikura can be tuned to some $\mathcal{M}_p$; in both cases, the rays actually land since the parameters are semi-hyperbolic. When a Julia set $\partial\mathcal{K}_{\widehat{c}}$ has Hausdorff dimension 2, an analogous paradoxon is obtained for dynamic rays landing at a small Julia set $\partial\mathcal{K}_c^p$.

3.3 Preimages and higher levels

For $c \in V_M$, the quadratic-like map $f_c^m : V_c \to U_c$ gives a compactly nested sequence of open sets, $U_c \supset V_c^0 = V_c \supset V_c^1 = V_c' \supset \dots$; now V_c' is connected since the critical value is $c \in V_c$, so we may consider the quadratic-like family $f_c^m : V_c' \to V_c$, $c \in V_M$, instead. According to [18], there is a nested sequence of parapuzzle-pieces $V_M^0 = V_M \supset V_M^1 = V_M' \supset \dots$ and a small Mandelbrot set $\mathcal{M}_m \subset V_M$, which shall be called the tiny Mandelbrot set associated to $\mathcal{M}_p$ and $\mathcal{K}_M^{m,p}$. It is primitive, since V_M' does not contain a hyperbolic component of period strictly dividing m. We shall construct embedded Julia sets of levels $l \ge 1$ with $\mathcal{K}_M^{l\cdot m,p} \subset V_M^{l-1} \setminus \overline{V_M^l}$. Here $\mathcal{K}_M^{1\cdot m,p} = \mathcal{K}_M^{m,p}$ and examples of $\mathcal{K}_M^{2\cdot m,p}$ and $\mathcal{K}_M^{3\cdot m,p}$ are shown in Figures 8 and 12. — The following Theorem 3.6 continues the analytic techniques from Proposition 3.1; it applies, e.g., to the puzzle-pieces constructed combinatorially in Theorem 3.3, but similarly to the round disks constructed analytically in [8, 21].

Theorem 3.6 (Higher levels, following Douady et alii)
Consider a small Mandelbrot set $\mathcal{M}_p$ and an embedded Julia set $\mathcal{K}_M^{m,p} \subset V_M$ according to Proposition 3.1, and the quadratic-like family $f_c^m : V_c' \to V_c$, $c \in V_M$:

1. *There is a unique primitive small Mandelbrot set $\mathcal{M}_m \subset V_M$ of period m, which shall be called the* ***tiny Mandelbrot set*** *in reference to $\mathcal{M}_p$ and $\mathcal{K}_M^{m,p}$. It is the intersection of a countable family of compactly nested parapuzzle-pieces $V_M^0 = V_M \supset V_M^1 = V_M' \supset \dots$; for $c \in V_M^n$, V_c^{n+1} is a disk moving holomorphically.*

2. *For $l \geq 1$ and $c \in V_{\scriptscriptstyle M}$ define $\mathcal{K}_c^{l\cdot m,p} := \{z \in V_c^{l-1} \,|\, f_c^{lm}(z) \in \mathcal{K}_c^p\} \subset \partial\mathcal{K}_c$. When $c \in V_{\scriptscriptstyle M}^{l-1}$, this map is a 2^l-to-1 cover and $\mathcal{K}_c^{l\cdot m,p}$ moves holomorphically.*

3. *The **embedded Julia set of level** $l \geq 1$ is the corresponding subset of the parameter plane, $\mathcal{K}_{\scriptscriptstyle M}^{l\cdot m,p} := \{c \in V_M \,|\, c \in \mathcal{K}_c^{l\cdot m,p}\} \subset \partial\mathcal{M}$. This Cantor set satisfies $\mathcal{K}_{\scriptscriptstyle M}^{l\cdot m,p} \subset V_{\scriptscriptstyle M}^{l-1} \setminus \overline{V_{\scriptscriptstyle M}^l}$ and it is a quasiconformal image of $\mathcal{K}_c^{l\cdot m,p}$ for any $c \in V_{\scriptscriptstyle M}^{l-1}$.*

Proof: We have $\mathcal{K}_c^{m,p} \subset V_c \setminus \overline{V_c'}$ and $\mathcal{K}_{\scriptscriptstyle M}^{m,p} \subset V_{\scriptscriptstyle M} \setminus \overline{V_{\scriptscriptstyle M}'}$, since $f_c^m(\overline{V_c'}) \subset \overline{V_c}$ and $\overline{V_c} \cap \mathcal{K}_c^p = \emptyset$. Using the base point $c_* = c_m$, the Słodkowsky Theorem 2.2 gives a holomorphic motion $i_c^1 : \mathbb{C} \to \mathbb{C}$, $c \in V_{\scriptscriptstyle M}$, which agrees with the composition of Boettcher maps $\Phi_c^{-1} \circ \Phi_*$ on $\partial V_* \cup \partial V_*'$ and with the motion of $\mathcal{K}_c^{m,p}$ according to Proposition 3.1.2. Now for $c \in V_{\scriptscriptstyle M}'$ there is a holomorphic motion $i_c^2 : \overline{V_*'} \setminus V_*'' \to \overline{V_c'} \setminus V_c''$ with $f_c^m \circ i_c^2 = i_c^1 \circ f_*^m$ there; extend it to $z \in \mathbb{C} \setminus \overline{V_*'}$ as $i_c^2(z) = i_c^1(z)$ and to $z \in V_*''$ arbitrarily. Note that i_c^1 and i_c^2 match continuously on $\partial V_*'$, since $f_c^m \circ i_c^1 = i_c^1 \circ f_*^m$ there, and that $i_c^2 : \mathcal{K}_*^{2\cdot m,p} \to \mathcal{K}_c^{2\cdot m,p}$ by equivariance. The holonomy $h_2 : V_{\scriptscriptstyle M}' \to V_*'$ with $h_2(c) = (i_c^2)^{-1}(c)$ is quasiconformal according to Proposition 2.3, and it satisfies $h_2 : \mathcal{K}_{\scriptscriptstyle M}^{2\cdot m,p} \to \mathcal{K}_*^{2\cdot m,p}$. As in the proof of Proposition 3.1, the base point $*$ may be changed temporarily, and Misiurewicz points are dense in $\mathcal{K}_{\scriptscriptstyle M}^{2\cdot m,p}$. — The same arguments are used recursively to construct i_c^l, h_l, $\mathcal{K}_c^{l\cdot m,p}$, and $\mathcal{K}_{\scriptscriptstyle M}^{l\cdot m,p}$ for $c \in V_{\scriptscriptstyle M}^{l-1}$, $l > 2$. ∎

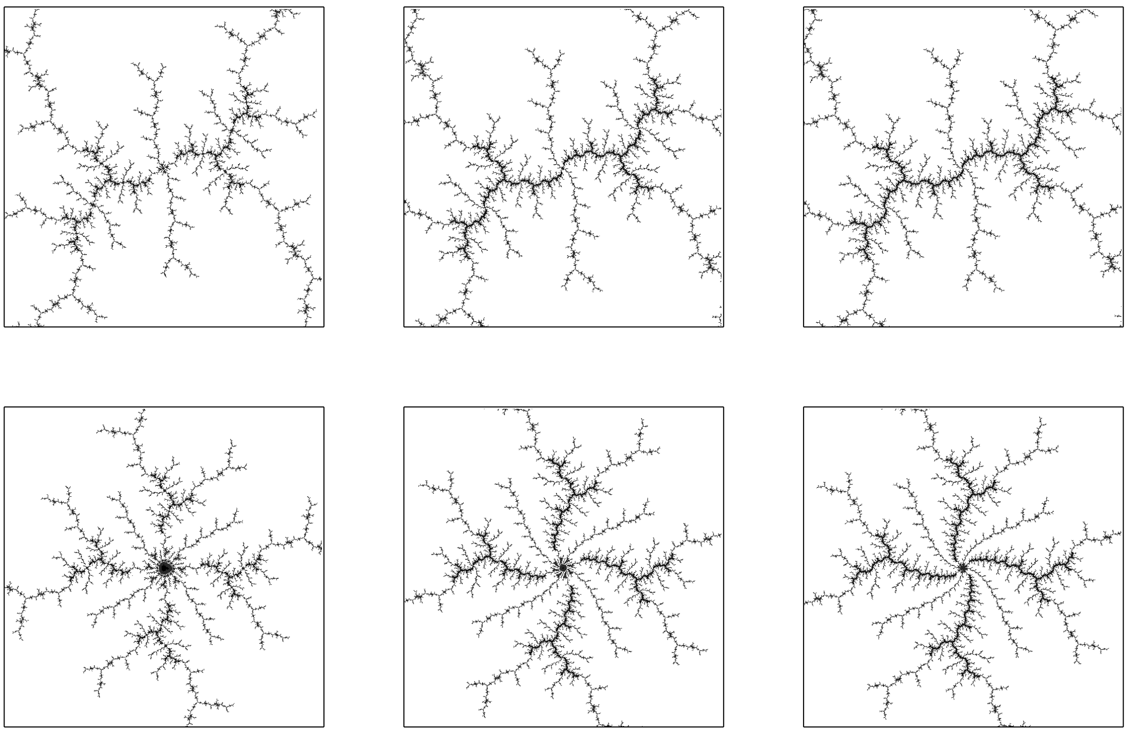

Figure 8: For the Misiurewicz point $a \in \mathcal{M}_4$ with the external angles 769/3840 and 783/3840, there is a sequence of centers $c_{m_n} \to a$ with $(m_n) = (11, 15, 19, \ldots)$. Illustrating asymptotic similarity according to Propositions 4.2 and 4.3, the images show embedded Julia sets $\mathcal{K}_{\scriptscriptstyle M}^{l\cdot m_n,4} \subset \partial\mathcal{M}$ with $m_n = 23, 35, 47$ rescaled and rotated by powers of the repelling multiplier ρ_a.
Top: $\rho_a^n \cdot (\mathcal{K}_{\scriptscriptstyle M}^{1\cdot m_n,4} - c_{m_n})$ converges to a conformal copy of $\mathcal{K}_a^p - \omega_a^p$.
Bottom: $\rho_a^{3/2\,n} \cdot (\mathcal{K}_{\scriptscriptstyle M}^{2\cdot m_n,4} - c_{m_n})$ converges to a conformal copy of $\sqrt{\mathcal{K}_a^p - \omega_a^p}$; note that convergence is slower on the second level.

Let us denote the straightening map of $\mathcal{M}_m$ by $\chi_\xi : c \mapsto \check{c}$ for $c \in V_{\scriptscriptstyle M}$, since $c \mapsto \widehat{c}$ was used for $\mathcal{M}_p$. The tubing is a quasiconformal map between annuli, $\xi_c : \overline{V_c} \setminus V_c' \to \overline{\mathbb{D}_{R^2}} \setminus \mathbb{D}_R$ conjugating f_c^m to $F(z) = z^2$ on the boundary, with $\xi_c \circ i_c^1 = \xi_*$ [5, 18]. The Straightening Theorem constructs a unique hybrid-equivalence ψ_c from f_c^m to $f_{\check{c}}$, such that $\psi_c = \Phi_{\check{c}}^{-1} \circ \xi_c$ on the fundamental annulus. This holds for any $c \in V_{\scriptscriptstyle M}$, but when $c \in V_{\scriptscriptstyle M} \setminus V_{\scriptscriptstyle M}'$ it gives an explicit description of χ_ξ as $\Phi_{\scriptscriptstyle M}(\check{c}) = \xi_*(h_1(c))$. This relation remains valid for $c \in V_{\scriptscriptstyle M} \setminus \mathcal{M}_m$, when $\xi_* : V_* \setminus \mathcal{K}_*^m \to \overline{\mathbb{D}_{R^2}} \setminus \mathbb{D}_1$ is extended appropriately and $h_n(c) = (i_c^n)^{-1}(c)$ is used. There is no analogous formula for $\chi_\xi : \mathcal{M}_m \to \mathcal{M}$, which is independent of the chosen $R > 1$ and ξ.

Remark 3.7 (Model set, Douady et alii)
Since the same holomorphic motions i_c^n and holonomy maps h_n are used to construct the straightening maps and the embedded Julia sets, the formulas above give the following quasiconformal model sets:

$$\psi_c \;:\; \mathcal{K}_c^m \cup \bigcup_{l=1}^{\infty} \mathcal{K}_c^{l\cdot m,\,p} \;\;\mapsto\;\; \mathcal{K}_{\check{c}} \cup \Phi_{\check{c}}^{-1}\Big(\bigcup_{l=1}^{\infty} F^{-(l-1)}\Big(\xi_*(\mathcal{K}_*^{m,\,p})\Big)\Big)\;, \tag{5}$$

$$\chi_\xi \;:\; \mathcal{M}_m \cup \bigcup_{l=1}^{\infty} \mathcal{K}_{\scriptscriptstyle M}^{l\cdot m,\,p} \;\;\mapsto\;\; \mathcal{M} \cup \Phi_{\scriptscriptstyle M}^{-1}\Big(\bigcup_{l=1}^{\infty} F^{-(l-1)}\Big(\xi_*(\mathcal{K}_*^{m,\,p})\Big)\Big) \tag{6}$$

with $F(z) = z^2$ and the extended tubing ξ_* for the center $c_* = c_m$ of $\mathcal{M}_m$. Note that (5) is valid in this form for $c \in \mathcal{M}_m$ only, but it remains valid in $V_{\scriptscriptstyle M}$ for suitable finite unions. A quasiconformal copy of the model set is constructed in [8, 21] by replacing $\xi_*(\mathcal{K}_*^{m,\,p})$ with $\mathcal{K}_{\widehat{c_*}}$, rescaled to fit into the round annulus $\mathbb{D}_{R^2} \setminus \overline{\mathbb{D}_R}$.

For each tiny Mandelbrot set $\mathcal{M}_m$, the embedded Julia sets $\mathcal{K}_{\scriptscriptstyle M}^{l\cdot m,\,p}$ are contained in a single decoration of $\mathcal{M}_p$; we shall see in Proposition 3.11 how this decoration determines the geometry of $\mathcal{K}_{\scriptscriptstyle M}^{m,\,p}$. The following result concerns the decorations of $\mathcal{M}_m$, which are labeled by dyadic angles according to Theorem 2.5.2:

Proposition 3.8 (Decorations of the tiny Mandelbrot set)
Consider embedded Julia sets $\mathcal{K}_{\scriptscriptstyle M}^{l\cdot m,\,p}$ of different levels l, surrounding a tiny Mandelbrot set $\mathcal{M}_m$ according to Theorem 3.6.

a) If $\mathcal{M}_p$ is primitive and $\mathcal{M}_m$ is before $\mathcal{M}_p$, then $\mathcal{K}_{\scriptscriptstyle M}^{m,\,p} = \mathcal{K}_{\scriptscriptstyle M}^{1\cdot m,\,p}$ is contained in the $1/4$- and $3/4$-decorations of $\mathcal{M}_m$. So $\mathcal{K}_{\scriptscriptstyle M}^{l\cdot m,\,p}$ meets a decoration of denominator 2^k, if and only if $k = l + 1$.

b) Suppose $\mathcal{M}_m$ is not before $\mathcal{M}_p$, so it is behind $\mathcal{M}_p$ or located in a branch or sublimb at the vein before $\mathcal{M}_p$. Then $\mathcal{K}_{\scriptscriptstyle M}^{m,\,p} = \mathcal{K}_{\scriptscriptstyle M}^{1\cdot m,\,p}$ is contained in the $0/1$- and $1/2$-decorations of $\mathcal{M}_m$. Thus $\mathcal{K}_{\scriptscriptstyle M}^{l\cdot m,\,p}$ meets a decoration of denominator 2^k, if and only if $k \le l$.

Proof: a) Suppose $\mathcal{M}_m$ is before $\mathcal{M}_p$ und consider $\mathcal{K}_c^{m,\,p}$ for $c = c_m$. Then f_c^m maps both the $1/4$- and the $3/4$-decoration of $\mathcal{K}_c^m$ 1-to-1 to the $1/2$-decoration, which contains $\mathcal{K}_c^p$. So both decorations contain a subset of $\mathcal{K}_c^{m,\,p}$, and both subsets together are all of $\mathcal{K}_c^{m,\,p}$, since this set is mapped 2-to-1 to $\mathcal{K}_c^p$. — Now let the parameter $c \in V_{\scriptscriptstyle M}$ vary, then $\mathcal{K}_c^{m,\,p}$ cannot cross the boundary of the $1/4$- and $3/4$-carrots of $\mathcal{K}_c^m$, which consists of rays and boundary points of $\mathcal{K}_c^m$; these carrots persist or they are merged to a strip, which still contains $\mathcal{K}_c^{m,\,p}$. Since $c \in \mathcal{K}_{\scriptscriptstyle M}^{m,\,p} \Leftrightarrow c \in \mathcal{K}_c^{m,\,p}$, the embedded Julia set is contained in the $1/4$- and $3/4$-carrots of $\mathcal{M}_m$

as well. The statement for higher levels l follows by taking preimages of dynamic decorations under f_c^m.

b) Again, consider $\mathcal{K}_c^{m,p}$ for $c = c_m$. Any decoration of $\mathcal{K}_c^m$ with denominator $> 2^1$ is mapped injectively by f_c^m to a decoration of denominator $\geq 2^1$ behind $\mathcal{K}_c^m$, which does not meet $\mathcal{K}_c^p$. The 1/2- and the 0/1-decorations, intersected with V_c, are mapped injectively by f_c^{m-1} to two sets symmetric to 0, so both must meet $f_c^{-1}(\mathcal{K}_c^p)$. Note that when $\mathcal{M}_m$ is behind $\mathcal{M}_p$, the main vein through $\mathcal{K}_c^m$ meets $\mathcal{K}_c^{m,p}$, since $f_c^{-1}(\mathcal{K}_c^p)$ intersects the spine $[-\beta_c, \beta_c] \subset \mathcal{K}_c$. On the other hand, when there is a branch point separating α_c, $\mathcal{K}_c^m$, and $\mathcal{K}_c^p$, its preimages under f_c^m are two branch points on the main vein through $\mathcal{K}_c^m$, and $\mathcal{K}_c^{m,p}$ is contained in branches off the vein. — In both cases, the 1/2- and 0/1-carrots intersected with $\overline{V_c} \setminus V_c'$ do not branch as $c \in V_M$ varies, so the same statements apply to $\mathcal{K}_M^{m,p}$. ∎

Example 3.9 (Tuning by tiny Mandelbrot set)
Suppose $\mathcal{M}_{m'}$ is a primitive small Mandelbrot set of period $m' > p$, close to $\mathcal{M}_p$ and such that $\mathcal{K}_M^{m',p}$ exists. Then consider the tuned Airplane $\mathcal{M}_m$, which is a primitive small Mandelbrot set $\mathcal{M}_m \subset \mathcal{M}_{m'}$ with $m = 3m'$. The $\pm 7/16$-decorations of $\mathcal{M}_{m'}$ are contained in the $\pm 1/4$-decorations of $\mathcal{M}_m$. If $\mathcal{M}_{m'}$ is before $\mathcal{M}_p$, these decorations contain $\mathcal{K}_M^{1\cdot m,p}$, which is a subset of $\mathcal{K}_M^{3\cdot m',p}$. On the other hand, if $\mathcal{M}_{m'}$ is behind $\mathcal{M}_p$, these decorations contain a subset of $\mathcal{K}_M^{4\cdot m',p}$ but $\mathcal{K}_M^{1\cdot m,p}$ does not exist: otherwise further levels are obtained in Theorem 3.6 and there is a sequence of Misiurewicz points approaching the root of $\mathcal{M}_m$ from before it, such that the period is p and the preperiod grows by m. This sequence is eventually contained in $\mathcal{M}_{m'}$, so all periods and preperiods must be divisible by m', contradicting $m' > p$. See also Remark 3.2.

According to the definition in Proposition 3.1 and Theorem 3.6, a compact subset $\mathcal{K} \subset \partial\mathcal{M}$ is an embedded Julia set $\mathcal{K}_M^{l\cdot m,p}$, if there are stable puzzle-pieces V_c with certain mapping properties. Then there will be several possible choices for V_c. On the other hand, $\mathcal{K}_M^{m,p}$ determines $\mathcal{M}_p$ and $\mathcal{M}_m$ uniquely; probably for $\mathcal{M}_p$ and $\mathcal{M}_m$ there will be at most one $\mathcal{K}_M^{l\cdot m,p}$ for each l. See also Remark 3.2.

Remark 3.10 (Significance of puzzle-pieces)
A parameter c with $f_c^{l\cdot m}(c) \in \mathcal{K}_c^p$ need not belong to any embedded Julia set $\mathcal{K}_M^{l\cdot m,p}$, and a subset $\mathcal{K} \subset \partial\mathcal{K}_c$ mapped 2^l-to-1 to $\mathcal{K}_c^p$ by $f_c^{l\cdot m}(z)$ need not be of the form $\mathcal{K}_c^{l\cdot m,p}$ either: pathological examples are ruled out by requiring a puzzle-piece V_c or V_c^{l-1}, see also Remark 3.14.2. E.g., we cannot take half of $\mathcal{K}_M^{2\cdot m,p}$ and consider it as a $\mathcal{K}_M^{1\cdot 2m,p}$. And in the following Section 3.4 we shall see that $\mathcal{K}_M^{m,p} = \mathcal{K}_M^{1\cdot m,p}$ is a union of two embedded Julia sets of preperiod $m+p$, four of preperiod $m+2p$ ...; again, this decomposition is not arbitrary: e.g., taking two of the four embedded Julia sets of preperiod $m+2p$, their union need not give one of preperiod $m+p$.

3.4 Structure of embedded Julia sets

This section is concerned mainly with the structure of embedded Julia sets $\mathcal{K}_M^{m,p} = \mathcal{K}_M^{1\cdot m,p}$ in terms of channels and nodes. The interested reader may obtain a corresponding description of higher levels $\mathcal{K}_M^{l\cdot m,p}$ around $\mathcal{M}_m$. Remark 3.14 gives an informal discussion of further embedded sets around the nodes. — We shall relate the structure of $\mathcal{K}_M^{m,p}$, $\mathcal{K}_c^{m,p}$, and $\mathcal{K}_c^p$ to the Cantor Julia set $\mathcal{K}_{\widehat{c}}$, where $\widehat{c}$ is a parameter on a dyadic external ray. Now the dyadic dynamic ray through the critical value $z = \widehat{c}$ has two preimages, which are meeting and branching at the critical point $z = 0$; these provide a subdivision of $\mathcal{K}_{\widehat{c}}$ into two halves. Taking iterated preimages under $f_{\widehat{c}}$ gives a recursive subdivision by ray pairs branching at precritical points. These branched ray pairs correspond to channels in the complement of $\mathcal{K}_M^{m,p}$, and to connecting arcs within $\mathcal{M}$ bridging the channels.

Proposition 3.11 (Channels and nodes)
In the situation of Proposition 3.1, consider the nested open sets U_c^n with $U_c^0 = U_c$ and $f_c^p : U_c^n \to U_c^{n-1}$, and suppose that no ∂U_c^n intersects V_c for $c \in V_M$; this condition is always satisfied by the constructions in the proof of Theorem 3.3. The embedded Julia set of the first level, $\mathcal{K}_M^{m,p} = \mathcal{K}_M^{1,m,p} \subset \mathcal{M}$ is described as follows:

1. *For each order $k \ge 0$, $\mathcal{K}_M^{m,p}$ has a dynamically natural subdivision into 2^k subsets, each of which is an embedded Julia set $\mathcal{K}_M^{m+kp,p}$ of preperiod $m+kp$. The corresponding tiny Mandelbrot sets $\mathcal{M}_{m+kp}$ are called **nodes of order** k.*
2. *When $\mathcal{M}_m$ is behind $\mathcal{M}_p$, the channels between these subsets correspond to merged carrots of $\mathcal{K}_c^p$ and to crashing rays of $\mathcal{K}_{\widehat{c}}$, cf. Figures 9 and 13. Here c is an arbitrary parameter in the decoration of internal angle θ containing $\mathcal{K}_M^{m,p}$, and $\widehat{c}$ is any parameter on the dyadic ray of angle θ. Likewise, the nodes of order k correspond to preimages of ω_c^p under f_c^{kp} and to preimages of 0 under $f_{\widehat{c}}^k$, respectively.*

The embedded Julia sets $\mathcal{K}_M^{m,p}$ of order 0 in Figures 2, 8 top, and 10 left look symmetric and similar to quadratic Julia sets. This is no longer the case for higher orders, e.g., considering the two halves $\mathcal{K}_M^{m+p,p}$ of $\mathcal{K}_M^{m,p}$. Since all of these are constructed from Proposition 3.1, what is the difference? The examples have been chosen such that the modulus of $V_c \setminus \overline{V_c'} \supset \mathcal{K}_c^{m,p}$ is relatively large, and the conformal map $f_c^{m-1} : \mathcal{K}_c^{m,p} \to f_c^{-1}(\mathcal{K}_c^p)$ has small distortion. On the other hand, $f_c^{m-1}(\mathcal{K}_c^{m+p,p})$ is half of $f_c^{-1}(\mathcal{K}_c^p)$, and this half is mapped to the symmetric set $f_c^{-1}(\mathcal{K}_c^p)$ by a conformal restriction of f_c^p, which seems to have higher distortion.

Proof: Un UMn connected . twice as many vertices and decorations, see figures, notation decos . locally when not primitive or different choice . above construction in segment, maybe not always but assumed . so V in single segment in deco of angle theta

1. recursive subdivision of Uc then Vc, holomotion and holonomy and VM . why tiny not within . either apply recursively or at once . nodes in channels . stability within segment and partly deco
2. geometry recursive merging as for hat c, also lamination . connecting arcs ■

for impl-cauli also 0 and 1/2-carrots merged in first step, then looks different because of infinite crossings since 0-ray is periodic . image easy from hat c gt 0, tessellation [7] p. 133, [20]

Probably Munafo [31] was the first to define nodes and to describe the geometry of connecting arcs, see also [37, 38, 12]. He conjectured the following accumulation statement:

Proposition 3.12 (Accumulation of nodes, following Munafo)
In the situation of Proposition 3.11, the nodes form a countable family of tiny Mandelbrot sets. The Cantor set $\mathcal{K}_M^{m,p}$ is the accumulation set of this family, in the sense that: for every $c \in \mathcal{K}_M^{m,p}$ there is a sequence of distinct nodes, which converges to

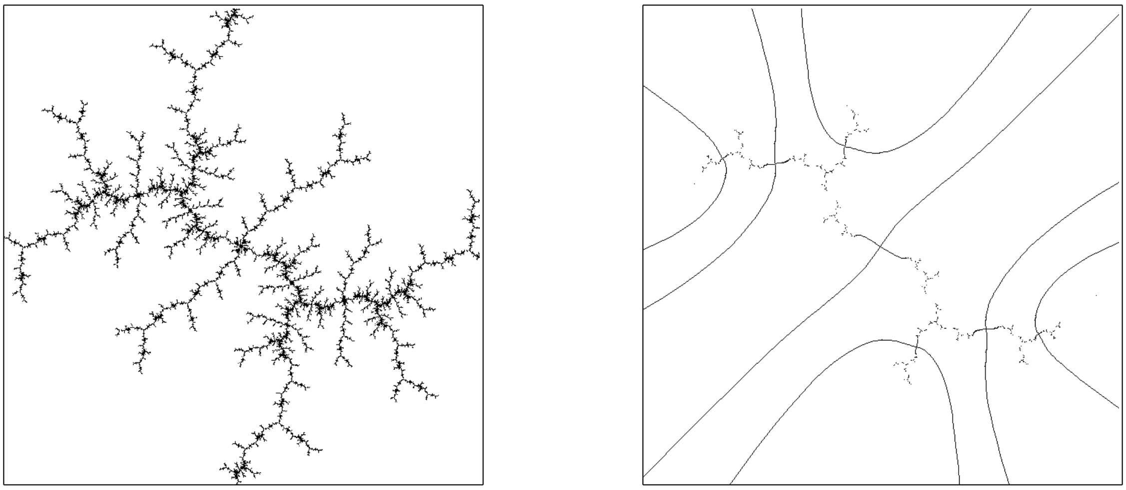

Figure 9: Left: the embedded Julia set $\mathcal{K}_M^{23,\,4} \subset \partial\mathcal{M}$, rotated by 60°.
Right: the Cantor Julia set $\mathcal{K}_{\widehat{c}}$ for a parameter $\widehat{c}$ on the ray $\mathcal{R}_M(1/4)$, cf. Figure 1.
Note that the connecting components of $\mathcal{M} \setminus \mathcal{K}_M^{23,\,4}$ follow the same pattern as the crashing binary rays of $\mathcal{K}_{\widehat{c}}$, which are shown for preperiods ≤ 5. See also the carrots merged to strips in Figure 13.

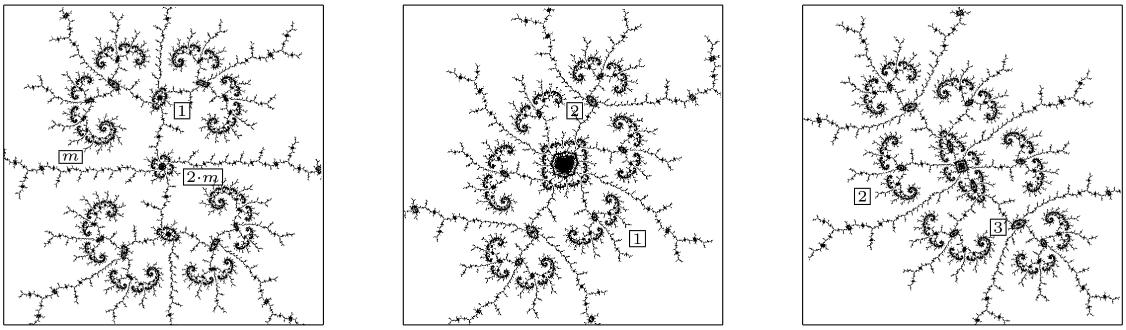

Figure 10: Left: an embedded Julia set $\mathcal{K}_M^{m,\,p} = \mathcal{K}_M^{35,\,4}$ of Cauliflower shape, located on the vein before the small Mandelbrot set $\mathcal{M}_p = \mathcal{M}_4$. The next level $\mathcal{K}_M^{2\cdot m,\,p}$ and the tiny Mandelbrot set $\mathcal{M}_m = \mathcal{M}_{35}$ are barely visible in the center. The elliptical cage around a node of first order is marked "1" and nodes of higher orders are visible but unmarked.
Middle and right: subsequent zooms reveal nested cages converging to a Misiurewicz point of preperiod 38 and period 35, cf. Remark 3.14.

$\{c\}$ with respect to the Hausdorff metric. And conversely, every accumulation point of such a sequence belongs to $\mathcal{K}_M^{m,\,p}$.

Proof: nested curves move holomorphically — estimate modulus ∎

The periodic binary expansion of angles can be written as $.\overline{u_\pm}$ for the angles of $\mathcal{M}_p$ and $.\overline{v_\pm}$ for the angles of $\mathcal{M}_m$, where $u_\pm$ are words of p digits and $v_\pm$ have m digits. For various examples, Romera et alii [37, 38] have observed a pattern of appended binary digits for external angles of nodes, see also [12]:

Proposition 3.13 (Angles of nodes, following Romera et alii)
In the situation of Proposition 3.11, each node $\mathcal{M}_{m+kp}$ has two $(m+kp)$-periodic external angles at its root. For technical reasons, let as assume in addition that there is a strip $\widetilde{V}_M$ with $\mathcal{K}_M^{m,\,p} \subset \overline{\widetilde{V}_M}$, such that f_c^{m-1} is injective on corresponding strips

$\widetilde{V}_c$. *Then for any order $k \ge 0$ the 2^k nodes $\mathcal{M}_{m+kp}$ have external angles of the form $.\overline{v_\pm u_1 \dots u_k}$ with $u_i \in \{u_-, u_+\}$.*

Proof: follow orbit relative to spine, note usually rays in both ends of the channel, only before exception at order 0 . case without additional assumption . concrete angles from initial digits at hat c, or ordered counterclockwise ∎

Finally, let us turn to a few observations on embedded Julia sets of higher levels and around the nodes: For $c \in V_M$, consider two polynomial-like maps in a neighborhood of $z = 0$, $f_c^p : f_c^{-1}(U_c') \to f_c^{-1}(U_c)$ and $f_c^m : f_c^{-1}(V_c) \to f_c^{-1}(U_c)$. Taking iterated preimages of $f_c^{-1}(\mathcal{K}_c^p)$ with respect to the union of these two maps gives a countable family of subsets of $\mathcal{K}_c$, whose preimages in V_c under f_c^{m-1} may correspond to subsets of $\mathcal{M}$.

Taking preimages only with respect to f_c^m corresponds to embedded Julia sets $\mathcal{K}_M^{l\cdot m,\,p}$ of higher levels around $\mathcal{M}_m$, while taking preimages of these with f_c^p gives structures around the nodes $\mathcal{M}_{m+kp}$. These are shown in Figure 10 for an example with $\mathcal{K}_M^{1\cdot m,\,p}$ of Cauliflower shape; here the structures are reckognized easily as elliptical cages. When the parameter c is close to the node $\mathcal{M}_{m+p}$ and to the cage marked "1", the critical value $f_c^{m-1}(c)$ is relatively far outside of $f_c^{m-1}(\mathcal{K}_c^{2\cdot m,\,p}) = f_c^{-m}(f_c^{-1}(\mathcal{K}_c^p))$, so this set has an elongated shape. One of its two preimages under f_c^p is a cage around $f_c^{m-1}(c)$, whose preimage around c corresponds to the cage "1".

Remark 3.14 (Nested structures of various levels and orders)
1. Looking at higher levels $f_c^{m-1}(\mathcal{K}_c^{l\cdot m,\,p}) = f_c^{-(l-1)m}(f_c^{-1}(\mathcal{K}_c^p))$, in each step we get two smaller cages within each cage of the previous level. By taking preimages with f_c^p and f_c^{m-1} once, we are back around $z = c$ and see a corresponding family of nested cages in the parameter plane: "1" around the node $\mathcal{M}_{m+p}$, "2" and its cousin around small Mandelbrot sets of period $2m+p$, "3" and three cousins around Mandelbrot sets of period $3m+p$ …; choosing a sequence appropriately gives convergence to a Misiurewicz point of preperiod $m+p-1$ and period m, and rescaled cages converge to a limit set. — Zooming into the parameter plane at this Misiurewicz point is quite interesting due to the infinite sequence of these Cantor sets, which look similar to nested closed curves. See, e.g., www.mndynamics.com/vids/misi38_35nested.mp4

2. Here the cage "1" around the node $\mathcal{M}_{m+p}$ corresponds to a subset of $\mathcal{K}_c$, which is mapped 4-to-1 to $\mathcal{K}_c^p$ by f_c^{2m+p}. This is not an embedded Julia set. It turns out that the middle half of the cage is an embedded Julia set of the second level $\mathcal{K}_M^{2\cdot(m+p),\,p}$ around $\mathcal{M}_{m+p}$. Now consider the upper half of the cage "1", which surrounds the tiny Mandelbrot set of period $2m+p$ within the cage "2". This structure corresponds to a subset of $\mathcal{K}_c$, which is mapped 2-to-1 to $\mathcal{K}_c^p$ by f_c^{2m+p}. So it behaves like an embedded Julia set of the first level, $\mathcal{K}_M^{1\cdot(2m+p),\,p}$, but it does not satisfy the assumptions of Proposition 3.1: a para-puzzle-piece V_M intersects $\mathcal{M}$ in a connected set, and connecting arcs show that this set must contain a subset of $\mathcal{M}_{m+p}$. Then corresponding puzzle-pieces V_c contain $\mathcal{K}_c^{m+p}$, and f_c^{2m+p} is not 2-to-1 on V_c. Moreover, there are not two suitable primitive nodes of order one, with period $(2m+p)+1\cdot p$. See also Remarks 3.2 and 3.10.

These structures are favorite subjects for zoom movies and fractal art pictures [23]. A great variety of shapes can be sculpted by zooming deeply into $\mathcal{M}$, repeatedly choosing different levels and orders of embedded Julia sets, sometimes switching to a small Mandelbrot set outside of some structure to find that structure doubled. See, e.g., [32, 13] and the references therein.

4 Relation to various similarity phenomena

incl cf as / loc with each other and with embed

4.1 Homeomorphisms

incl. ren, when renormalizable, on edges and at Misi, moving only Mm or both, edge contains embedded. at primitive roots, homeos and asymptotic geometry are not known.

Proposition 4.1 ()

Proof: ■

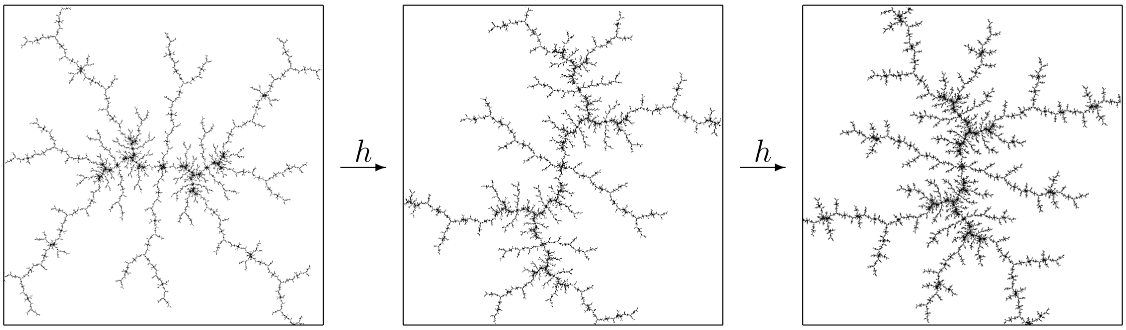

Figure 11: The homeomorphism $h : \mathcal{E}_M \to \mathcal{E}_M$ is contracting at $a = \gamma_M(11/56) = \gamma_M(15/56)$ and expanding at $b = \gamma_M(23/112) = \gamma_M(29/112)$; h^{-1} was the standard example in [17]. The three images show subsets of the Mandelbrot set mapped to each other by h, located in the 1/3-sublimbs and 1/4-decorations of the primitive Mandelbrot sets $\mathcal{M}_p$ with external angles 26/127 and 33/127, 3/15 and 4/15, 25/127 and 34/127. Embedded Julia sets are mapped as $\mathcal{K}_M^{32,\,7} \mapsto \mathcal{K}_M^{23,\,4} \mapsto \mathcal{K}_M^{38,\,7}$.

4.2 Asymptotic similarity

see Figure 8 top given above. [43, 35]

Proposition 4.2 ()

Proof: ■

4.3 Asymptotics on multiple scales

see Figure 8 bottom given above

Proposition 4.3 ()

Proof: ∎

4.4 Local similarity

see Figure 12

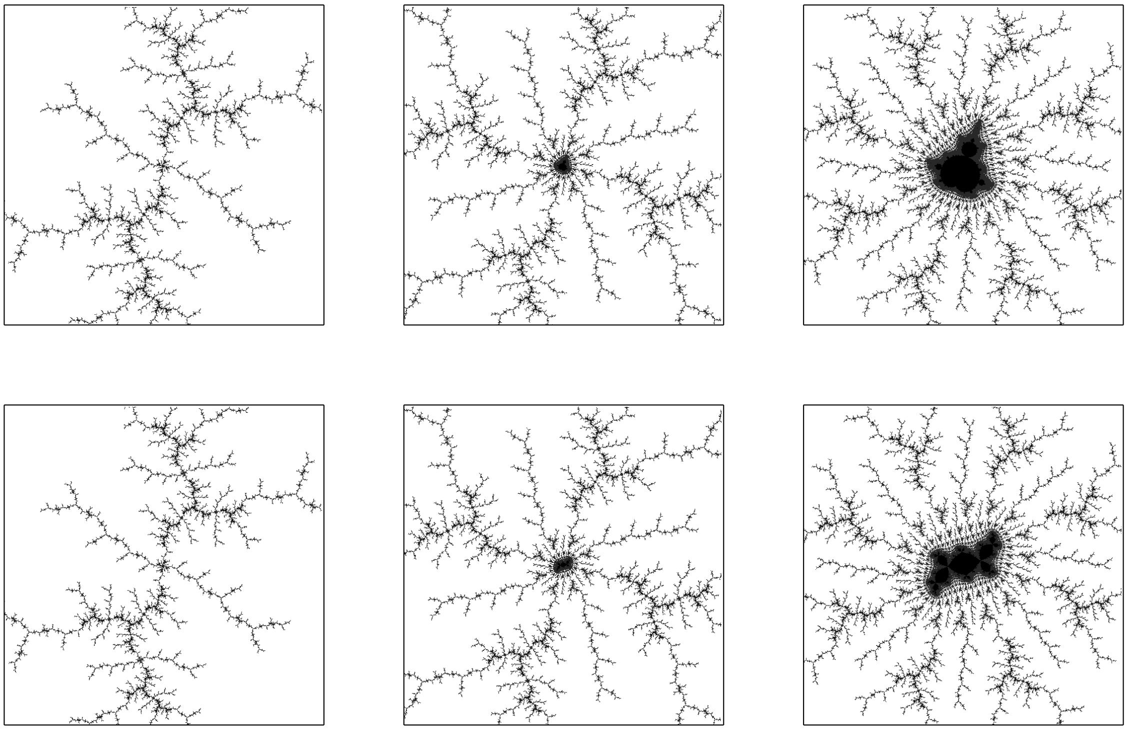

Figure 12: Top: successive zooms around our tiny Mandelbrot set $\mathcal{M}_{23}$ showing embedded Julia sets $\mathcal{K}_M^{l\cdot 23,\,4}$ of levels $l = 1,\,2,\,3$.
Bottom: local similarity is illustrated by corresponding zooms in the dynamic plane of the tuned Rabbit c of period $23 \cdot 3$, rescaled with the similarity factor λ.

Proposition 4.4 ()

Proof: ∎

A Remarks on computer graphics

esctime, comparison, dist estimate [30], and Marty, both unsatisfactory at small M sets, see Figure 5, probably subpixel-supersampling would be better. Figure?

for renormalization (primitive) and with preperiod.

note embedded often easy to recognize with escape time, even when widely disconnected, is actually artifact since filaments are barely visible: large neighborhood of embedded in the same color range, only few pixels of the same color in the filaments

note embedded visible in part because whole pixels are colored, in part because of decorations

problem with satellite renormalization: not too close to root, not automatically

B Holomorphic motions and renormalization

This is a preview of material from [18].

Recall the statement of **Proposition 2.3:**
Suppose $U_M \subset \mathbb{C}$ is a Jordan disk and for c in a neighborhood $\widetilde{U}_M \supset \overline{U_M}$, $i_c : \mathbb{C} \to \mathbb{C}$ is a holomorphic motion with base point $c_* \in U_M$. For a holomorphic $f : \widetilde{U}_M \to \mathbb{C}$ define the holonomy map $h : \widetilde{U}_M \to \mathbb{C}$ with $h(c) = i_c^{-1}(f(c))$. Assume that there is a Jordan disk U_*, such that $h : \partial U_M \to \partial U_*$ is an orientation-preserving homeomorphism. Then $h : U_M \to U_*$ is quasiconformal.

The map h may be regarded as the holonomy between the transversal manifolds $\{(c, z) \,|\, z = f(c)\}$ and $\{(c, z) \,|\, c = c_*\}$ along the leaves $\{(c, z) \,|\, z = i_c(z_0)\}$ of the fibration defined by the holomorphic motion i_c. The proof follows Lyubich [25, 26]; similar techniques were used by Shishikura to estimate the Hausdorff dimension in [41], and for smooth holomorphic motions the result is due to Douady–Hubbard [5].

Proof: $i_c^{\pm 1}(z)$ is jointly continuous and $h(c)$ is continuous. It has discrete fibers, since for any z, the equation $i_c(z) = f(c)$ is analytic in c and h is not constant. To obtain estimates of $z = h(c)$ at $z_0 = h(c_0)$, introduce new coordinates $w(z) = i_{c_0}(z)$ and set $w_0 = i_{c_0}(z_0) = f(c_0)$. Then

$$\Big(i_c \circ i_{c_0}^{-1}\Big)(w) - i_c(z_0) = f(c) - i_c(z_0) \tag{7}$$

and for $c \approx c_0$ we may expand both sides as

$$(w - w_0) + a_{c,\,w} \cdot (c - c_0) = b \cdot (c - c_0)^n \cdot \Big(1 + \mathcal{O}(c - c_0)\Big) \tag{8}$$

with suitable $n \in \mathbb{N}$ and $b \neq 0$. Here $a_{c,\,w}$ is obtained by taking the derivative of the left hand side of (7) with respect to c, replacing c with $c_0 + t(c - c_0)$, and integrating from $t = 0$ to 1. Now the dilatation of $i_c \circ i_{c_0}^{-1}$ is small and the Hölder exponent is almost 1; the Cauchy inequality gives $a_{c,\,w} = \mathcal{O}(|w - w_0|^{1-1/(2n)})$. Then

$$\begin{aligned} w - w_0 &= b \cdot (c - c_0)^n \cdot \Big(1 + \mathcal{O}(\sqrt{c - c_0})\Big) \qquad \text{and} & (9)\\ h(c) &= i_{c_0}^{-1}\Big(f(c_0) + b \cdot (c - c_0)^n \cdot \Big(1 + \mathcal{O}(\sqrt{c - c_0})\Big)\Big) & (10)\end{aligned}$$

for $c \approx c_0$. This shows that the degree of $h(c)$ is positive at every $c_0 \in \widetilde{U}_M$ and moreover, h is an open map. So $h(\overline{U_M}) \subset \overline{U_*}$, $h(U_M) = U_*$, and $h : U_M \to U_*$ is proper. The global degree is 1 on ∂U_M, $\overline{U_M}$, and U_M, and it is the sum of the local degrees for all points c_0 in a fiber $h^{-1}(z_0)$. Thus $h : U_M \to U_*$ is a homeomorphism and for every $c_0 \in U_M$ we have $n = 1$ in (10).

For some $1 \le K < \infty$ and all $c \in \overline{U_M}$, $i_c^{\pm 1}$ is K-quasiconformal. Now (10) gives pointwise regularity properties as well: $h(c)$ is differentiable at $c = c_0$, if and only if $i_{c_0}^{-1}(w)$ is differentiable at $w = f(c_0)$, and then the dilatation of an infinitesimal circle is the same. However, it is not obvious that this is the case for almost every $c_0 \in U_M$, and that the weak derivatives of h exist. So we shall consider an alternative characterization of quasiconformal maps, which is based on small circles instead of infinitesimal circles: according to [10, 24], $i_{c_0}^{-1}$ satisfies

$$\limsup_{\delta \to 0} \frac{\max_{|w - w_0| = \delta} |i_{c_0}^{-1}(w) - i_{c_0}^{-1}(w_0)|}{\min_{|w - w_0| = \delta} |i_{c_0}^{-1}(w) - i_{c_0}^{-1}(w_0)|} \le K \tag{11}$$

for almost every w_0 and $\le \lambda(K) \le \exp(\pi K)$ everywhere. Then (10) gives

$$\limsup_{\delta \to 0} \frac{\max_{|c-c_0|=\delta} |h(c) - h(c_0)|}{\min_{|c-c_0|=\delta} |h(c) - h(c_0)|} \le \exp(\pi K) \tag{12}$$

for all $c_0 \in U_{M}$ and therefore h is $\exp(\pi K)$-quasiconformal on U_{M} .

Refined estimates of $\lambda(K)$ from [24] show that the dilatation bound of h goes to 1 as $K \to 1$. Actually, h is K-quasiconformal on U_{M} , but this is not straightforward to prove with the present approach: again, the problem is that for all c_0 , (11) is valid for almost all w_0 , but we need it for $w_0 = f(c_0)$ and almost all c_0 . In [36] an alternative proof is given by approximating i_c with a smooth holomorphic motion; this is possible according to [1]. ■

The hypothesis $\overline{U_{M}} \subset \widetilde{U}_{M}$ is needed, because otherwise the dilatation of h may blow up at ∂U_{M} . Moreover, in the following example we have $i_c^{\pm 1}(z) = z$ for $z \in \partial\mathbb{D}$, $c \in \mathbb{D}$, but a strict inclusion $h(\mathbb{D}) \subset \mathbb{D}$:

Example B.1 (Boundary behavior of h)
For $c \in \mathbb{D}$, a holomorphic motion i_c of $\mathbb{C}$ is given by

$$i_c(z) = z \cdot \exp\Big(\frac{2c}{1-c} \log|z|\Big) \qquad i_c^{-1}(z) = z \cdot \exp\Big(2\frac{|c|^2 - c}{1-|c|^2} \log|z|\Big)$$

for $z \in \mathbb{D}$ and $i_c(z) = z$ for $z \in \mathbb{C} \setminus \mathbb{D}$. The map $h(c) = i_c^{-1}(c)$ is a diffeomorphism on $\mathbb{D}$, and it extends to a homeomorphism on $\overline{\mathbb{D}}$. Although $i_c^{-1}(z) = z$ for $z \in \partial\mathbb{D}$ and $c \in \mathbb{D}$, the extended h is not the identity on $\partial\mathbb{D}$: we have $h(c) \sim c\,\mathrm{e}^{c-1}$ as $c \to \partial\mathbb{D}$. If $\mathcal{K}_c = i_c([-1/2,\, 0])$ and $\mathcal{K}_{M} = \{c \in \mathbb{D} \,|\, c \in \mathcal{K}_c\}$, then $\mathcal{K}_{M} = (-1,\, 0]$ is not compact and $h(\mathcal{K}_{M}) = (-\mathrm{e}^{-2},\, 0] \ne \mathcal{K}_0$.

To illustrate the notion of carrots and decorations in the case of a primitive small Mandelbrot set $\mathcal{M}_p$, let us start with the dynamics for parameters $c \in \mathcal{M}_p$. explain construction and properties of carrots and decorations, see Figure 13. start with dynamic decorations for c in Mp, then behind, later with strips and before primitive Mp.

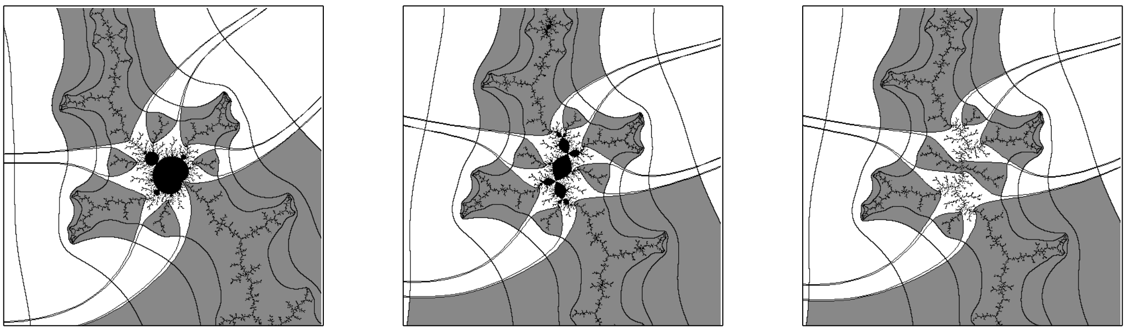

Figure 13: Left: parameter decorations of $\mathcal{M}_4$ in carrots (sectors).
Middle: corresponding dynamic decorations and carrots for $c \in \mathcal{M}_4$.
Right: for c in the 1/4-decoration, the dynamic carrots 1/8 and 5/8 merge to a strip.

Douady [7] considered the continuity of Julia sets depending on the polynomial. The analogous result for small Julia sets was employed in the proof of Theorem 3.3.3:

Proposition B.2 (Continuity of small Julia sets)
In the cases of primitive or satellite renormalization with $g_c = f_c^p : U_c' \to U_c$, *consider the convergence of small filled Julia sets* $\mathcal{K}_c^p$ *and of small strict Julia sets* $\partial\mathcal{K}_c^p$ *as* $c \to a \in U_{\scriptscriptstyle M}$ *:*

1. *For* $\varepsilon > 0$ *there is a* $\delta > 0$, *such that* $\mathcal{K}_c^p$ *is contained in an* ε*-neighborhood of* $\mathcal{K}_a^p$ *and* $\partial\mathcal{K}_a^p$ *is contained in an* ε*-neighborhood of* $\partial\mathcal{K}_c^p$, *when* $|c - a| < \delta$.

2. *We have* $\mathcal{K}_c^p \to \mathcal{K}_a^p$ *and* $\partial\mathcal{K}_c^p \to \partial\mathcal{K}_a^p$ *in the Hausdorff topology as* $c \to a$, *except in these cases:*

a) If $a \in \partial\mathcal{M}_p$ *is parabolic, then* $\mathcal{K}_c^p$ *and* $\partial\mathcal{K}_c^p$ *are not continuous at* $c = a$.

b) If $a \in \partial\mathcal{M}_p$ *is a Siegel parameter, then* $\mathcal{K}_c^p$ *is continuous at* $c = a$ *but* $\partial\mathcal{K}_c^p$ *is not.*

Proof: 1. In the primitive case, the set $\{(c,\, z) \,|\, z \in \mathcal{K}_c^p\} = \bigcap\{(c,\, z) \,|\, z \in g_c^{-n}(\overline{U_c'})\}$ is closed in $U_{\scriptscriptstyle M} \times \mathbb{C}$, thus $\mathcal{K}_a^p$ cannot expand suddenly for $c \approx a$. In the satellite case, a similar argument works within a subwake, or using the pre-renormalization. On the other hand, $\partial\mathcal{K}_a^p$ cannot suddenly contract, since it is covered by a finite collection of $\varepsilon/2$-neighborhoods of repelling periodic points. There is a $\delta > 0$ such that these are moving at most by $\varepsilon/2$ for $|c - a| < \delta$.

2. If $\partial\mathcal{K}_a^p = \mathcal{K}_a^p$, item 1 implies continuity of $\mathcal{K}_c^p$ and $\partial\mathcal{K}_c^p$ at $c = a$. If a is a hyperbolic parameter, then $\partial\mathcal{K}_c^p$ is moving holomorphically for $c \approx a$.

a) For a parabolic parameter $a \in \partial\mathcal{M}_p$, there is a sequence $c_n \to a$ such that $\widehat{c}_n \to \widehat{a}$ has the following properties according to [7]: $\partial\mathcal{K}_{\widehat{c}_n} = \mathcal{K}_{\widehat{c}_n} \to \mathcal{L}$, where the compact limit set satisfies $\partial\mathcal{K}_{\widehat{a}} \subset \mathcal{L} \subset \mathcal{K}_{\widehat{a}}$, and $\widehat{c}_n$ can be chosen such that these inclusions are proper, $\mathcal{L}$ has no interior, and it is not the boundary of a full set. Passing to a subsequence, there is a quasiconformal map ψ such that $\psi_{c_n}^{\pm 1} \to \psi^{\pm 1}$ locally uniformly, thus $\partial\mathcal{K}_{c_n}^p = \mathcal{K}_{c_n}^p = \psi_{c_n}^{-1}(\mathcal{K}_{\widehat{c}_n}) \to \psi^{-1}(\mathcal{L})$. Now we have $\partial\mathcal{K}_a^p \subset \psi^{-1}(\mathcal{L}) \subset \mathcal{K}_a^p$ by item 1, and these inclusions are proper by the topological properties of $\psi^{-1}(\mathcal{L})$.

b) Suppose $a \in \partial\mathcal{M}_p$ is a Siegel parameter and $c_n \to a$. Then $\widehat{c}_n \to \widehat{a}$ and $\psi_{c_n}(\mathcal{K}_{c_n}^p) = \mathcal{K}_{\widehat{c}_n} \to \mathcal{K}_{\widehat{a}} = \psi_a(\mathcal{K}_a^p)$ by [7]. Assume that $\mathcal{K}_{c_n}^p \not\to \mathcal{K}_a^p$. By item 1 there is an $\varepsilon > 0$ and a subsequence, such that $\mathcal{K}_a^p$ is not contained in the ε-neighborhood of $\mathcal{K}_{c_n}^p$. Passing to a subsequence again, we have $\mathcal{K}_{c_n}^p \to \psi^{-1}(\mathcal{K}_{\widehat{a}})$. Now $\psi^{-1}(\mathcal{K}_{\widehat{a}})$ is a proper subset of $\mathcal{K}_a^p$ and $\partial\mathcal{K}_a^p \subset \partial(\psi^{-1}(\mathcal{K}_{\widehat{a}}))$, which is a contradiction since $\mathcal{K}_{\widehat{a}}$ is full. Thus $\mathcal{K}_{c_n}^p \to \mathcal{K}_a^p$. Finally, choose $c_n \to a$ with $\partial\mathcal{K}_{c_n}^p = \mathcal{K}_{c_n}^p$, then $\partial\mathcal{K}_{c_n}^p \to \mathcal{K}_a^p \neq \partial\mathcal{K}_a^p$. ∎

References

[1] K. Astala, G. J. Martin, Holomorphic motions, in: *Papers on Analysis*, Report. Univ. Jyväskylä **83** (2001), pp. 27–40.

[2] X. Buff, C. Henriksen, Julia sets in parameter spaces, Comm. Math. Phys. **220**, 333–375 (2001).

[3] L. Carleson, T. W. Gamelin, *Complex dynamics*, Springer, New York, 1993.

[4] A. Douady, J. H. Hubbard, Étude dynamique des polynômes complexes, I, II, Publ. Math. d'Orsay 1984-2, 1985-4. www.math.cornell.edu/∼hubbard/OrsayEnglish.pdf

[5] A. Douady, J. H. Hubbard, On the dynamics of polynomial-like mappings, Ann. Sci. École Norm. Sup. **18**, 287–343 (1985).

[6] A. Douady, Algorithms for computing angles in the Mandelbrot set, in: *Chaotic Dynamics and Fractals*, Notes Rep. Math. Sci. Eng. **2**, 155–168 (1986).

[7] A. Douady, Does a Julia Set Depend Continuously on the Polynomial?, in: *Complex Dynamical Systems: The Mathematics behind the Mandelbrot and Julia Sets*, Proc. Symp. Appl. Math. **49**, AMS 1994.

[8] A. Douady, X. Buff, R. Devaney, P. Sentenac, Baby Mandelbrot sets are born in cauliflowers, in: *The Mandelbrot Set, Theme and Variations*, LMS Lecture Notes **274**, Cambridge 2000.

[9] D. Dudko, The decoration theorem for Mandelbrot and Multibrot sets, Int. Math. Res. Notices **2017**, 3985–4028 (2017).

[10] F. W. Gehring, The definitions and exceptional sets for quasiconformal mappings, Ann. Acad. Sci. Fenn. **A I 281**, 1–28 (1960).

[11] P. Haïssinsky, Modulation dans l'ensemble de Mandelbrot, in: *The Mandelbrot Set, Theme and Variations*, LMS Lecture Notes **274**, Cambridge 2000.

[12] C. Heiland-Allen, Navigating in the hairs, Patterns in embedded Julia sets, blog entries of 2014 and 2017.
http://mathr.co.uk/blog/2014-11-18_navigating_in_the_hairs.html
http://mathr.co.uk/blog/2017-11-06_patterns_in_embedded_julia_sets.html

[13] C. Heiland-Allen, Two spirals out ..., Efficient automated Julia morphing, blog entries of 2015 and 2017.
http://mathr.co.uk/blog/2015-05-18_two_spirals_out.html
http://mathr.co.uk/blog/2017-11-09_efficent_automated_julia_morphing.html

[14] J. H. Hubbard, *Teichmüller theory and applications to geometry, topology, and dynamics I: Teichmüller theory*, Matrix editions 2006.

[15] W. Jung, Mandel, interactive software. Asymptotic similarity is implemented since version 3.0 of 1999, local similarity since version 4.0 of 2007, embedded Julia sets and explanatory demos since version 5.3 of 2009. Available from www.mndynamics.com for Linux, Mac, and Windows.

[16] W. Jung, *Homeomorphisms on Edges of the Mandelbrot Set*, Ph.D. thesis RWTH Aachen University 2002. www.math.stonybrook.edu/ims-thesis-server

[17] W. Jung, Homeomorphisms of the Mandelbrot Set, in: *Dynamics on the Riemann Sphere*, A Bodil Branner Festschrift, EMS 2006, pp. 139–159.

[18] W. Jung, Primitive and satellite renormalization of quadratic polynomials, in preparation. See Appendix B.

[19] W. Jung, Local and asymptotic similarity between the Mandelbrot set and Julia sets, in preparation. See [16] and the slides www.mndynamics.com/papers/holbaek07a.pdf

[20] T. Kawahira, On the regular leaf space of the cauliflower, Kodai Math. J. **26**, 167–178 (2003).

[21] T. Kawahira, M. Kisaka, Julia sets appear quasiconformally in the Mandelbrot set, preprint (2018). arXiv:1804.00176

[22] B. Karpińska, Area and Hausdorff dimension of the set of accessible points of the Julia sets of $\lambda\exp(z)$ and $\lambda\sin(z)$, Fund. Math. **159**, 269–287 (1999).

[23] J. Leavitt, Leavittation, a series of images from 1998. See web.archive.org/web/20010112000300/http://www.sky-dyes.com/leavitt1.html

[24] O. Lehto, K. I. Virtanen, J. Väisälä, Contributions to the distortion theory of quasiconformal mappings, Ann. Acad. Sci. Fenn. **A I 273**, 1–14 (1959).

[25] M. Lyubich, Feigenbaum–Coullet–Tresser universality and Milnor's hairiness conjecture, Ann. Math. **149**, 319–420 (1999).

[26] M. Lyubich, *Conformal Geometry and Dynamics of Quadratic Polynomials, I–II*, in preparation. www.math.stonybrook.edu/∼mlyubich/papers/

[27] R. Mañé, P. Sad, D. Sullivan, On the dynamics of rational maps, Ann. Sci. École Norm Sup. **16**, 193–217 (1983).

[28] C. T. McMullen, *Complex Dynamics and Renormalization*, Annals of Mathematics Studies **135**, Princeton 1995.

[29] J. Milnor, Periodic Orbits, External Rays and the Mandelbrot Set: An Expository Account, Astérisque **261**, 277–333 (2000).

[30] J. Milnor, *Dynamics in One Complex Variable*, Annals of Mathematics Studies **160**, Princeton 2006.

[31] R. P. Munafo, Embedded Julia set, web page of 2008, with earlier versions since 1999. www.mrob.com/pub/muency/embeddedjuliaset.html

[32] R. P. Munafo, Reverse bifurcation, web page of 2002. www.mrob.com/pub/muency/reversebifurcation.html

[33] H.-O. Peitgen, D. Saupe, *The Science of Fractal Images*, Springer 1988.

[34] C. L. Petersen, P. Roesch, Carrots for dessert, Ergodic Th. Dyn. Syst. **32**, 2025–2055 (2012).

[35] J. Rivera-Letelier, On the continuity of Hausdorff dimension of Julia sets and similarity between the Mandelbrot set and Julia sets, Fund. Math. **170**, 287–317 (2001).

[36] P. Roesch, Holomorphic motions and puzzles (following M. Shishikura), in: *The Mandelbrot Set, Theme and Variations*, LMS Lecture Notes **274**, Cambridge 2000.

[37] M. Romera, G. Pastor, G. Álvarez, F. Montoya, External arguments of Douady cauliflowers in the Mandelbrot set, Computers & Graphics **28**, 437–449 (2004).

[38] M. Romera, G. Pastor, A. B. Orue, D. Arroyo, F. Montoya, Coupling Patterns of External Arguments in the Multiple-Spiral Medallions of the Mandelbrot Set, Discrete Dyn. Nature Society, Article ID 135637 (2009).

[39] D. Schleicher, Rational Parameter Rays of the Mandelbrot Set, Astérisque **261**, 405–443 (2000).

[40] D. Schleicher, On Fibers and Local Connectivity of Mandelbrot and Multibrot Sets, in: *Fractal geometry and applications*, Proc. Symp. Appl. Math. **72**, AMS 2004, 477–512.

[41] M. Shishikura, The Hausdorff Dimension of the Boundary of the Mandelbrot Set and Julia Sets, Ann. Math. **147**, 225–267 (1998).

[42] Z. Słodkowsky, Holomorphic motions and polynomial hulls, Proc. Am. Math. Soc. **111**, 347–355 (1991).

[43] Tan L., Similarity between the Mandelbrot set and Julia sets, Comm. Math. Phys. **134**, 587–617 (1990).